

MODELING AND SIMULATION OF CATALYTIC REVERSE FLOW REACTOR

A DISSERTATION

*Submitted in partial fulfillment of the
requirements for the award of the degree*

of

MASTER OF TECHNOLOGY

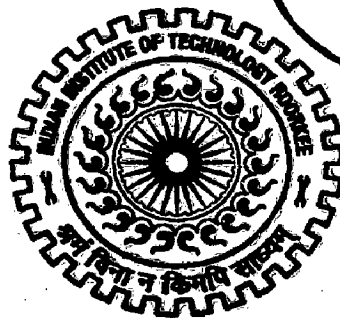
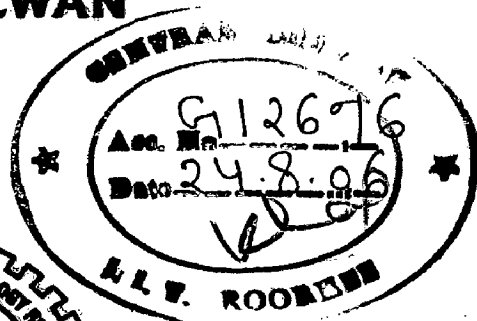
in

CHEMICAL ENGINEERING

(With Specialization in Industrial Safety and Hazards Management)

By

MOHD. RIZWAN



**DEPARTMENT OF CHEMICAL ENGINEERING
INDIAN INSTITUTE OF TECHNOLOGY ROORKEE
ROORKEE - 247 667 (INDIA)
JUNE, 2006**

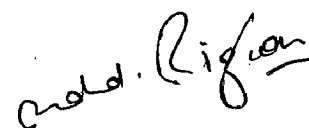
CANDIDATE'S DECLARATION

I, hereby, declare that the work which is being presented in the Dissertation entitled “**Modeling and Simulation of Catalytic Reverse Flow Reactor**” in partial fulfillment of the requirement for the award of the degree of Master of Technology in Chemical Engineering with specialization in **Industrial Safety and Hazards Management**, submitted in the Department of Chemical Engineering, Indian Institute of Technology Roorkee. This is an authentic record of my own work carried out during the period from July 2005 to June 2006, under the guidance of **Dr. Nidhi Bhandari**, Assistant Professor, Department of Chemical Engineering, Indian Institute of Technology Roorkee.

The matter embodied in this project work has not been submitted for the award of any other degree.

Date: 30 June, 2006

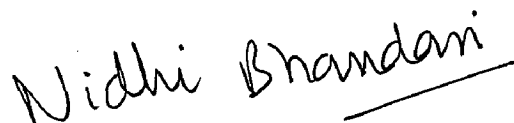
Place: IIT Roorkee.



(MOHD. RIZWAN)

CERTIFICATE

This is to certify that the above statement made by the candidate is correct to the best of my knowledge.



Dr. NIDHI BHANDARI
Assistant Professor,
Department of Chemical Engineering,
Indian Institute of Technology Roorkee

ACKNOWLEDGEMENT

I wish to express my sincere thanks and sense of gratitude to my project guide, Dr. Nidhi Bhandari, for her scholarly guidance, encouragement and discussion for this report. I am grateful to Dr. Sri Chand, HOD, Department of Chemical Engineering, IIT Roorkee, for providing me the necessary facilities for the compilation of this report.

I am indebted to all my colleagues, especially Suresh, Ganesh for their immense help and motivation in carrying out the literature survey and computational work related to this report.

Thanks are due to my friends Shoeb, Vivek, Fahad, Brijesh and Shushant for their indispensable help in the completion of this work. The Library In-charge, Mrs Verma, also deserve special thanks for placing the library at my disposal whenever required.

I am thankful to Mr. Salman Zafar and Mr. Asad Hasan Sahir for their unparalleled help and cooperation.

This report saw the light of the day only due to the encouragement and unflinching support and love of my parents, sisters and brothers.

Utmost thanks are due to the Almighty, for providing me the knowledge and wisdom for the successful completion of this report.

ABSTRACT

Polluted air can be decontaminated from volatile organic compounds by making use of catalytic oxidation in packed bed. Recently studies have exhibited that it can be profitable to apply an unsteady state process. A reverse flow reactor is an adiabatic packed bed reactor, which is forced to operate under transient conditions by reversing the direction of the feed flow periodically. The behavior of an adiabatic packed bed reactor with periodic flow reversal has been studied by means of modal calculations. By applying mass and heat balance heterogeneous model has been developed. The main advantage of applying this system for air purification process is an auto thermal process possible with low concentration of the contaminants in inlet and enables the reactor to handle fluctuations in inlet conditions like gas flow rate and concentration. The reactor could be operated auto thermally provided that the inlet concentrations were sufficiently high. If a mixture of contaminant is fed to the reactor is low then it might be necessary to increase total hydrocarbon concentration to assure an auto thermal process.

CONTENTS

Certificate	2
Acknowledgement	3
Abstract	4
List of Figures	7
Chapter 1. Introduction	11
Chapter 2. Literature Review	15
2.1 Removal of volatile organic compound from polluted air in reverse flow reactor: An experimental study	15
2.2 Catalytic combustion of very lean mixtures an a reverse flow reactor using an internal electrical heater	18
2.3 The catalytic oxidation of organic contaminants in a packed bed reactor	21
2.4 The spherical reverse flow reactor	22
2.5 A novel reverse flow reactor coupling endothermic and exothermic reactions: an experimental study	25
2.6 Catalytic partial oxidation of methane in a high-temperature reverse-flow reactor	27
2.7 Safety analysis of switching between reductive and oxidative conditions in reaction coupling reverse flow reactor	30
2.8 Reverse flow reactor operation and catalyst deactivation during high temperature catalytic partial oxidation	34
2.9 Pollutant destruction in a reverse flow chromatographic reactor	37
2.10 Flow-rate effects in flow-reversal reactors: experiments, simulations and approximations	39
2.11 Reverse flow catalytic burners: response to periodical variations in the feed	40

2.12 Multivariable model predictive control of a catalytic reverse flow reactor	43
Chapter 3. Mathematical Model	46
Chapter 4. Simulation of the Model	49
Chapter 5. Results and Discussions	53
Chapter 6. Conclusions and Recommendations	61
Nomenclature	63
References	65

LIST OF FIGURES

Figure 1.1	The reverse flow concept	13
Figure 2.1	Axial temp profiles	16
Figure 2.2	Conversion, maximum and mean outlet temperature as a function of the cycle number	17
Figure 2.3	Experimental axial temperature profiles for two different concentrations	19
Figure 2.4	Influence of the electrical power input on the axial temperature profiles	20
Figure 2.5	Schematic diagram of the spherical RFR model	23
Figure 2.6	Close up of the temperature profile for different internal radii	24
Figure 2.7	Effect of the flow rate on the conversion profiles	24
Figure 2.8	Schematic representation of the reaction coupling reverse flow reactor (RCRFR) concept for the catalytic non-oxidative propane dehydrogenation	26
Figure 2.9	CO selectivities, H ₂ selectivities, and CH ₄ conversions as a function of the CH ₄ O ₂ ratio for steady-state	28
Figure 2.10	Temperatures as a function of the CH ₄ O ₂ ratio	28
Figure 2.11	CO selectivities, H ₂ selectivities, and CH ₄ conversions as well as maximum and mean temperatures as a function of the cycling period $\tau/2$.	29

Figure 2.12	Catalyst temperatures as a function of the total volumetric gas flow	30
Figure 2.13	Axial mass fraction profiles after 0.05 sec. for the catalyst and gas phase in case of propane superseded with air without premixing in the inlet section	31
Figure 2.14	Temperature profile for the catalyst and gas phase in case of propane superseded with air without premixing in the inlet section	32
Figure 2.15	Effect of the channel diameter on the maximum gas temperature with no premixing in the inlet section	32
Figure 2.16	Catalyst and gas-phase axial temperature profiles at every 0.4 s when feeding a premixed propane/air mixture to a catalytic monolith	33
Figure 2.17	Schematic drawing of the reactor set-up	34
Figure 2.18	Direct comparison of hydrogen selectivities at steady state operation and reverse-flow operation for Pt, Rh and Ir.	35
Figure 2.19	Methane conversion, syngas selectivities and catalyst temperatures versus total volumetric inlet flow rate at steady-state reactor operation and reverse-flow operation for the Pt, Rh and Ir catalyst	36
Figure 2.20	Influence of the dimensionless adsorption capacity on the steady-state pollutant effluent concentration from a packed-bed reactor.	38

Figure 2.21	Experimental axial temperature profiles for flow reversal operation with various flow rates and feed concentration	40
Figure 2.22	Periodical variations in the inlet concentration	42
Figure 2.23	Fluctuations of the maximum temperature in the reactor, when the pseudo steady state has been reached.	42
Figure 2.24	Principle scheme for the catalytic reverse flow reactor	44
Figure 2.25	Spatial discretization in the reactor	45
Figure 4.1	Description of the finite difference method	50
Figure 5.1	Graph between temperature of gas and height of reactor at time = 0, 0.5, and 1	54
Figure 5.2	Graph between temperature of gas and height of reactor at time = 1.5, 2.0, and 2.5	55
Figure 5.3	Graph between concentration of gas and height of reactor	56
Figure 5.4	Graph between temperature of wall (at $x=0$ and 0.1) and time in first monolith in reactor	57
Figure 5.5	Graph between temperature of wall and time in first monolith in reactor (at $x=0.2$, 0.3 and 0.4	58
Figure 5.6	Graph between temperature of wall (at $x=0.85$ and 1) and time in second first monolith in reactor	59
Figure 5.7	Graph between temperature of wall (at $x=1.1$ and 1.2) and time in second first monolith in reactor	60
Figure 6.1	Improved principle scheme of catalytic reverse flow reactor	62

Dedicated

to

My

Parents

CHAPTER 1

INTRODUCTION

During the last decade environmental protection has received an increasing interest from the government and the industry. In the field of air pollution, the contaminant with volatile organic compound (Volatile organic compounds) is one of the problems. Some of these components are toxic by themselves, whereas most of them are precursors for the formation of ozone. Ozone is one of the key components in photochemical smog which is a well-known phenomenon especially during summer time. Under the influence of sunlight, Volatile organic compounds and NO_x can form a complex mixture, which is referred as photochemical smog. To prevent the occurrence of photochemical smog and the formation of ozone in the atmosphere, a reduction in Volatile organic compounds are required.

The primary method for the reduction of Volatile organic compounds emission into the atmosphere is source reduction. If this is not sufficient, more capital intensive method should be reviewed. The waste producing process should be redesigned in such a way that pollution is minimized and possible waste streams have to be taken care off or have to be purified. As far as treatment of polluted air is concerned, a large number of methods are available. The economically most attractive method depends on the specific condition of each case like the concentration and nature of the contaminants and air flow (van Riel, 1991).

In the case of valuable contaminants, separation method with recovery of the organics compounds might be considered. Examples in this area are membrane separation and pressure swing adsorption. The common feature of these methods is that during the first step of the process the contaminants are concentrated in a much smaller air stream. The second step is actual recovery of contaminants from the enriched air stream. Another group of purification methods are destructive processes like thermal and catalytic combustion. An advantage of these methods is the non selective behavior. For all these methods several modifications or combinations are possible.

In Novosibirsk, Russia, some decades ago, Boreskov and coworkers developed a new technology which can be applied to air purification problems (Boreskov *et al.* 1986).

The basic idea was that operating a reactor under transient condition can improve the performance of the reactor and in this particular case unsteady state condition is created by periodically reversing the direction of the feed flow. The benefits of operating a reactor under unsteady state condition have been summarized by Matros (1990). Westerterp (1992) referred to this reactor as a multifunctional reactor, because reactor and heat exchanger are integrated in one apparatus

Reverse Flow

Typical reactors, such as the fixed bed type often found in industry, are operated in a unidirectional manner. There is a fixed inlet and a fixed outlet. A reverse-flow reactor does not have a fixed inlet or outlet. The inlet is periodically switched between two sides of a reactor. Thermal energy generated in an exothermic reaction in a well-insulated unidirectional reactor is often lost to the outlet stream. Reverse-flow, a forced unsteady state process, is used to help utilize the thermal energy inside a reactor. Energy from the reaction and exit gasses are captured and utilized within the reactor by the reversing flow action. The captured thermal energy can be used to preheat the feed or be extracted from the reactor. This allows a reactor core to remain at high temperatures, even if the inlet feed is at lower, ambient temperatures.

The concept of reverse flow was not feasible up to 1950. Early issues with oscillations and dealing with the accumulation of thermal energy discouraged the technology at the time. With reverse flow, reactions that are not normally auto thermal may be run and sustained at lower inlet temperatures and higher conversions are possible than in a direct flow adiabatic reactor. A reverse-flow reactor may need some initial preheating to bring the catalyst to an acceptable temperature, but a well designed reactor should be able to thermally sustain itself once running. If similar equipment was used, but in unidirectional mode, the reaction typically would be self-extinguishing. As more feed gas enters the reactor and is preheated by the inlet inert section, the thermal energy stored in the inert section is depleted. Soon, the catalyst section begins to be cooled by the incoming gas and the reaction rate lowers. The reactor will have extinguished itself very quickly.

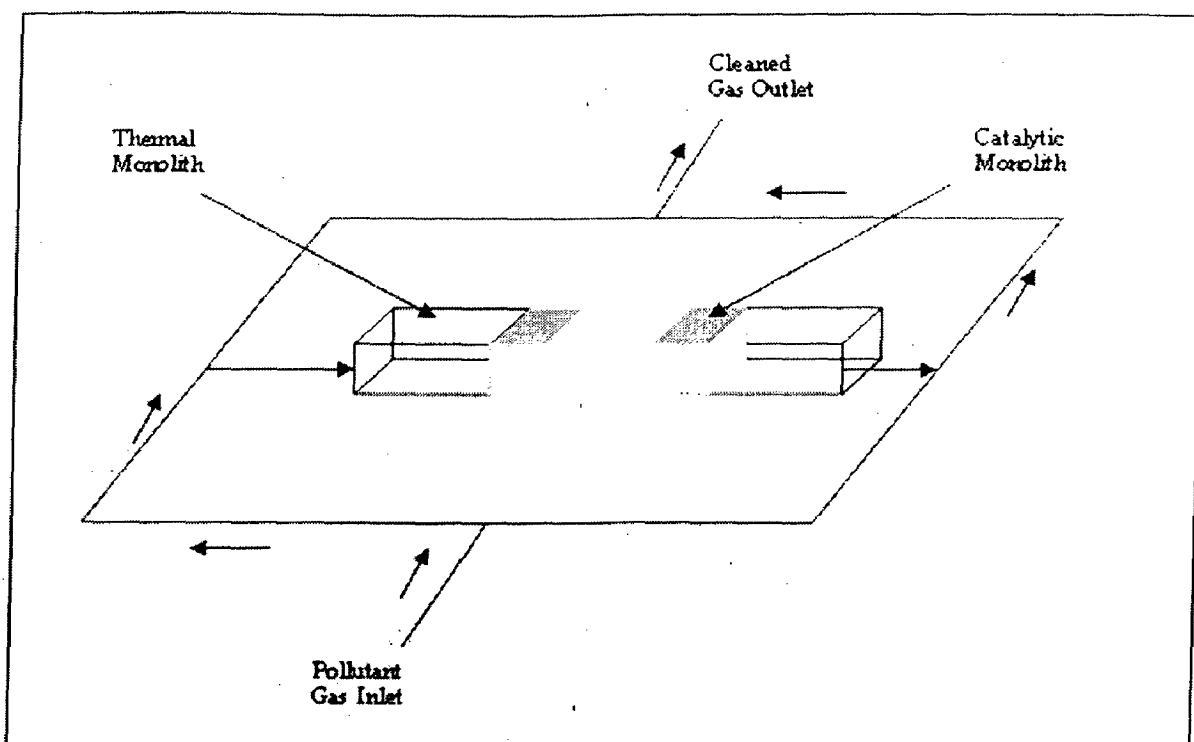


Figure 1.1: The reverse flow concept. For a determined length of time the reactor will operate in forward flow. After a definite length of time, the flow direction will be reversed. The open central section may be used for heat or gas extraction by providing an insulation layer.

In Figure 1.1, a schematic diagram of a reverse flow reactor is shown. At start-up the reactor bed is preheated to high temperature of around 300-400 °C. Subsequently the contaminated feed flow is fed to the reactor in ambient temperature. The gas flow is heated up by the hot solid phase and consequently the reactor bed will cool down which will result in the movement of heat front through the reactor towards the outlet. In the region of bed where the temperature is high enough i.e. above the ignition temperature of reaction, the oxidation reaction starts and on these positions the reaction heat is released. Because the ratio of heat capacities of the solid phase and gas phase is large it will take a rather long time before the heat front reaches the reactor outlet.

In recent years the distinct advantages of operating a reactor under non steady state condition have been demonstrated by Boreskov *et al.* (1986). They introduced the purification of waste air by catalytic oxidation in adiabatic packed bed reactor with periodic flow reversal. The reactor is thus operated under transient conditions. The packed bed act then as a regenerative heat exchange due to high heat capacity of the solid phase and, moreover, an auto thermal process is possible even at very low contaminant

concentrations. Other advantages of operating a process under transient condition are summarized by Matros (1990). Several authors have studied the applicability of a reverse flow reactor for the purification of waste air in Matros (1988), Eigenberger and Nieken (1988), Chumachenko and Matros (1990), and Sapundzhiev *et al.* (1991).

The behavior of an adiabatic packed bed reactor with periodic flow reversal has been studied by means of modal calculations. The model was proposed by Boroskov *et al.* (1979) further improved by van de Beld and Westerterp (1993). The packed bed acts as a regenerative heat exchanger due to high heat capacity of the solid phase and, moreover an auto thermal process possible even at very low contamination.

Model proposed by various authors is solved by different methods, e.g. van de Beld and Westerterp (1993) solution comprised of a set of partial differential equations converted into non linear ordinary differential equation and non linear algebraic equation. Now these equations can be solved by initial guess in solid phase temperature profile in the equation and whole process is repeated again until the difference between calculated and estimated value is very small.

In this work these equation is solved by MS EXCEL spread sheet. After solving equations various behaviors of temperature in the solid bed and in gas phase are obtained. The behaviors of the temperatures in solid as well as in gas phase obtained from with the help of different curves are investigated, such as, temperature of the gas rises in the first thermal monolith, and then destruction of the volatile organic compounds takes place in catalytic monolith followed by decrease in temperature of the gas in second thermal monolith. On the other hand for the solid phase, temperature falls in first thermal monolith and rises in second thermal monolith due to heat exchange with gas phase which have been investigated in detail.

CHAPTER 2

LITERATURE REVIEW

2.1 van de Beld *et al* (1994)

Removal of volatile organic compound from polluted air in reverse flow reactor: An experimental study

Van de Beld *et al* (1994) studied the reverse flow reactor for the purification of contaminated air. For this purpose, an experimental reactor was constructed which could be operated auto thermally provided that the inlet concentration of the pollutants were sufficiently high. To facilitate an auto thermal process, it might be necessary to increase the total hydrocarbon concentration. An increase in the mass flow rate will lead to high plateau temperature i.e. maximum temperature in the reactor core will increase. The reverse flow reactor, if operated on a large scale, will behave close to adiabatically, and therefore it is important to have adiabatic condition in the laboratory scale reactor. Blanks *et al.* (1990) recognized the problem of achieving adiabatic conditions in a laboratory scale reactor, and after some preliminary experiment they concluded that the reactor diameter should be increased. Applying a RFR for air cleaning makes an auto thermal process possible with low concentrations of the contaminants and enables the reactor to handle fluctuation in inlet concentration, as evident in industrial practice.

In this study, the experimental reactor has an inner diameter of 145 mm and a length of 1 meter, and the wall thickness is 1.6 mm. The reactor is equipped with an evacuated jacket; the total diameter is about 250 mm. In the reactor the temperature becomes rather high and therefore three radiation shields have been placed in annulus. The first 0.175 meter of the reactor is filled with inert α - Al_2O_3 pellets, which have negligible catalyst activity for the oxidation reactions as given in van de Beld and Westerterp (1994b). On this inert layer 0.65 meter of the catalyst, Pd/ Al_2O_3 is placed; above that the rest reactor filled with inert material. At 20 different axial positions the gas phase temperature is measured. Ethane, propane and methanol have been used as organic contaminants. The total hydrocarbon concentration is detected on-line with a FID analyzer. To obtain adiabatic condition, air is heated to a certain temperature and fed to the reactor. For these experiments the direction of feed flow is not reversed and in absence

of chemical reaction. Thus, for an adiabatic reactor operated under steady state condition the inlet and outlet temperature will be equal to each other.

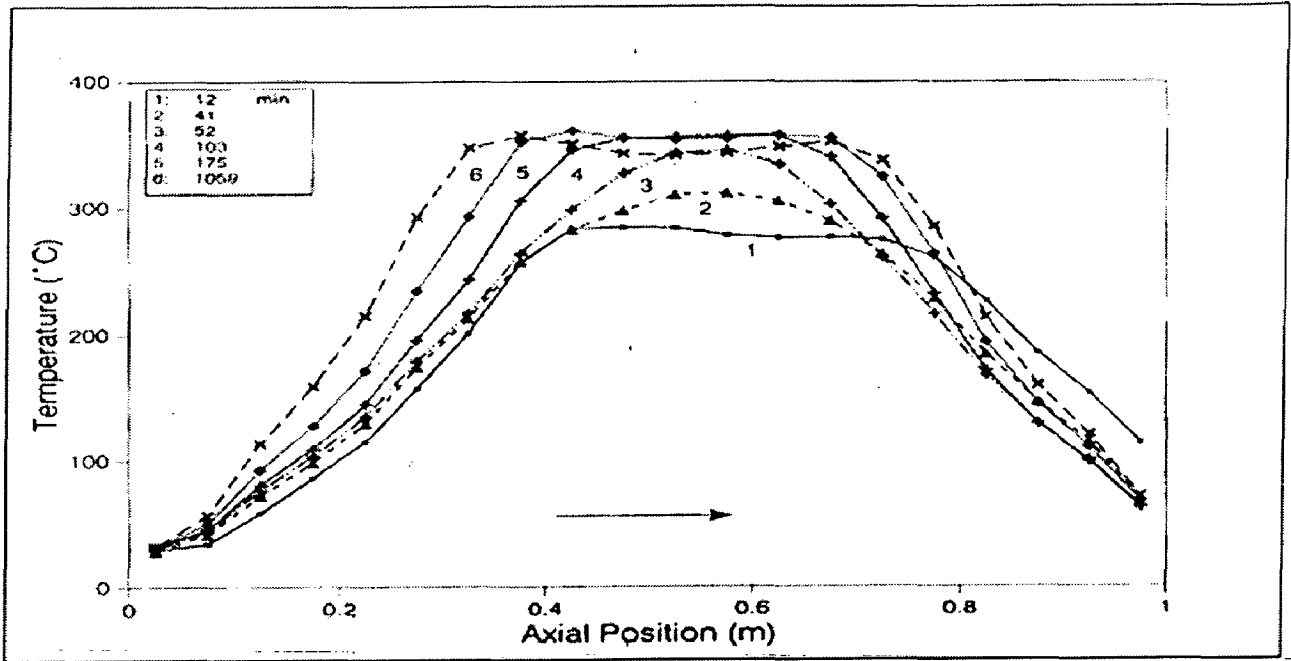


Figure 2.1: Axial temp profiles. $T_0 = 30^\circ\text{C}$, $t_c = 145\text{s}$; $C_{\text{ethane}} = 0.068 \text{ vol\%}$; $\Delta T_{ad} = 30.3^\circ\text{C}$

In Figures 2.1, for profile 1, the temperature is low; thus the chemical reaction is slow and reaction takes place in the centre of reactor. The conversion is about 75%. Initially, only temperature in the centre of the reactor will increase, because the reaction heat is released there (profile 2) and the profile will develop in inlet and outlet direction of the reactor. After a large period of time, the profile becomes constant over a cycle. In the steady state there is no accumulation of heat in the reactor; the reaction heat is removed from the reactor by convection via an increase in outlet temperature. For the experimental reactor a correction should be made for the heat losses: the following heat balance should hold

$$\bar{T}_{out} = \int_0^{(\frac{1}{2})t_c} T_{out}(t) dt = T_0 + \Delta T_{ad} - \Delta T_{lost} \quad (2.1)$$

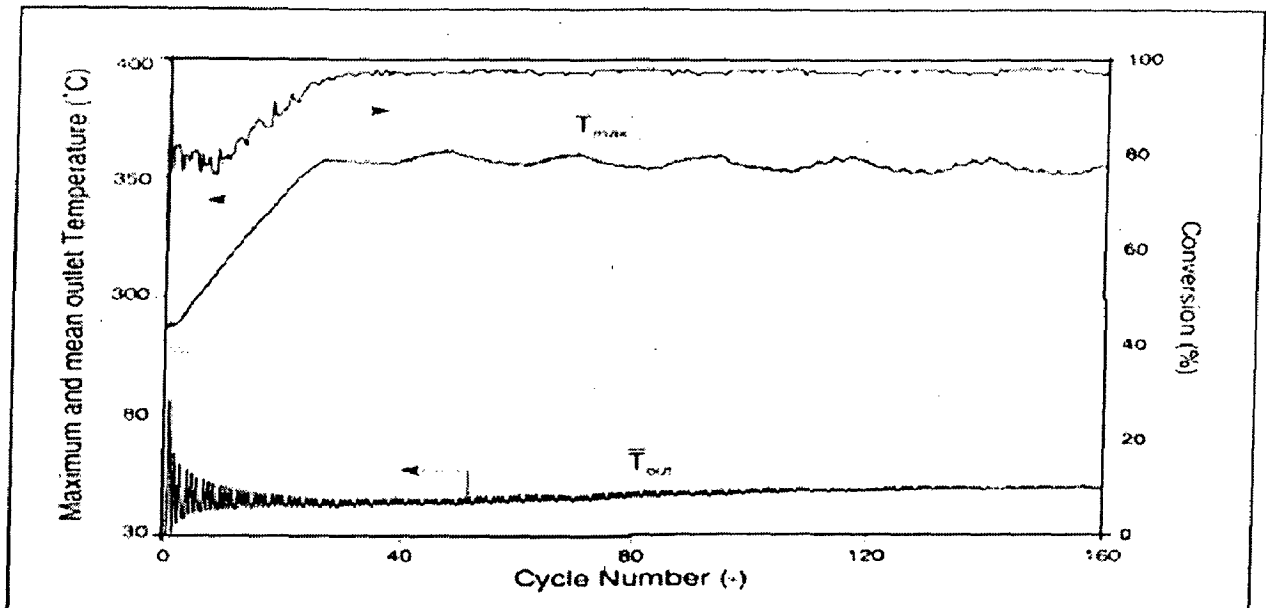


Figure 2.2: Conversion, Maximum and Mean Outlet Temperatures as a function of the cycle number.

We can conclude from Figure 2.2 that whether pseudo steady state is achieved, the mean outlet temperature is more significant parameter to follow than T_{max} or X , because as long as the temperature profiles are changing the mean outlet temperature will not be constant. For the experiment given in Figures 2.1 and 2.2, ΔT_{lost} is about 10°C , which corresponds with 30% of the reaction heat. The maximum temperature is almost insensitive to change in cycle period which is in good agreement with the results reported in literature. In all the cases, adiabatic temperature rise has been maintained at a constant value of $\Delta T_{ad} = 43^{\circ}\text{C}$. Ethane is easier to oxidize than propane and thus the oxidation of ethane is completed at lower temperatures as reported in van de Beld and Westerterp (1995). The temperature profiles for mixtures of propane and ethane are found between those of single components. If the inlet concentration becomes too low ΔT_{ad} reduces drastically and the temperature of the reactor will decrease and the reactor will be extinguished.

The purification of polluted air in reverse flow reactor has been studied experimentally. The influence of several operating parameters on the reactor behavior has been discussed. Although radial heat loss can not completely be excluded on small scale reactor, by making use of an evacuated jacket and several radiation shields the dynamic of the system is well defined and the heat losses are minimized. The reactor was operated successfully and high conversions of the contaminants were obtained without additional energy supply, provided that inlet concentrations were not too low. In case of different

components in the feed a total hydrocarbon concentration does not necessarily guarantee that all components individually achieve high conversions.

2.2 van de Beld *et al.* (1997)

Catalytic combustion of very lean mixtures in a reverse flow reactor using an internal electrical heater

This study is concerned with the experimental study of a reverse flow reactor, equipped with an internal electric heater, to treat lean feeds, in particular ethane, propane, and their mixtures. The influence of several operating parameters like electrical heater power, cycle period, chemical character, and concentration of pollutants on the maximum temperature and on the shape of temperature profile in the stationary state has been discussed. Results showed that an internal electrical heater can be successfully used to oxidize completely very lean mixture which would not be able to maintain an auto thermal process by themselves. The limiting concentration is usually specified in terms of the minimum adiabatic temperature rise, $\Delta T_{ad,min}$, given by the expression

$$\Delta T_{ad,min} = \frac{H_1 C_{1,min}^0}{(\rho c_p)_g^0} \quad (2.2)$$

Below this value the reverse flow reactor is extinguished, no reaction occurs and the maximum temperature is equal to feed temperature. The minimum adiabatic temperature rise depends on the efficiency of heat exchange and the ignition temperature, which is on reactive component and catalyst. Thus, it is a characteristic value for each system and, in general, for a well designed reverse flow reactor ranges from 10 °C to 30 °C

The experimental reactor consists of a tube, 1 meter in length and 145 mm in diameter. To avoid heat losses to the surroundings, the reactor was equipped with an evacuated jacket and four radiation shields. The front and rear part of the reactor was filled with inert material. Twenty thermocouples were placed in the reactor to measure gas temperature, and solid phase temperature was measured at 12 positions. In the middle of catalyst bed a standard electrical heater coil was placed. The power released by the heater was varied between 0 to 1000 Watt measures by an AC kWh meter. The total hydrocarbon

concentration in the inlet and outlet for the reactor was detected on-line by FID analyzer.

The mathematical model consists of three energy balances for the catalyst, the wall, and the gas and as many mass balances for solid and gas phases as there are components. To solve the model a finite difference technique has been applied using 300 grid points.

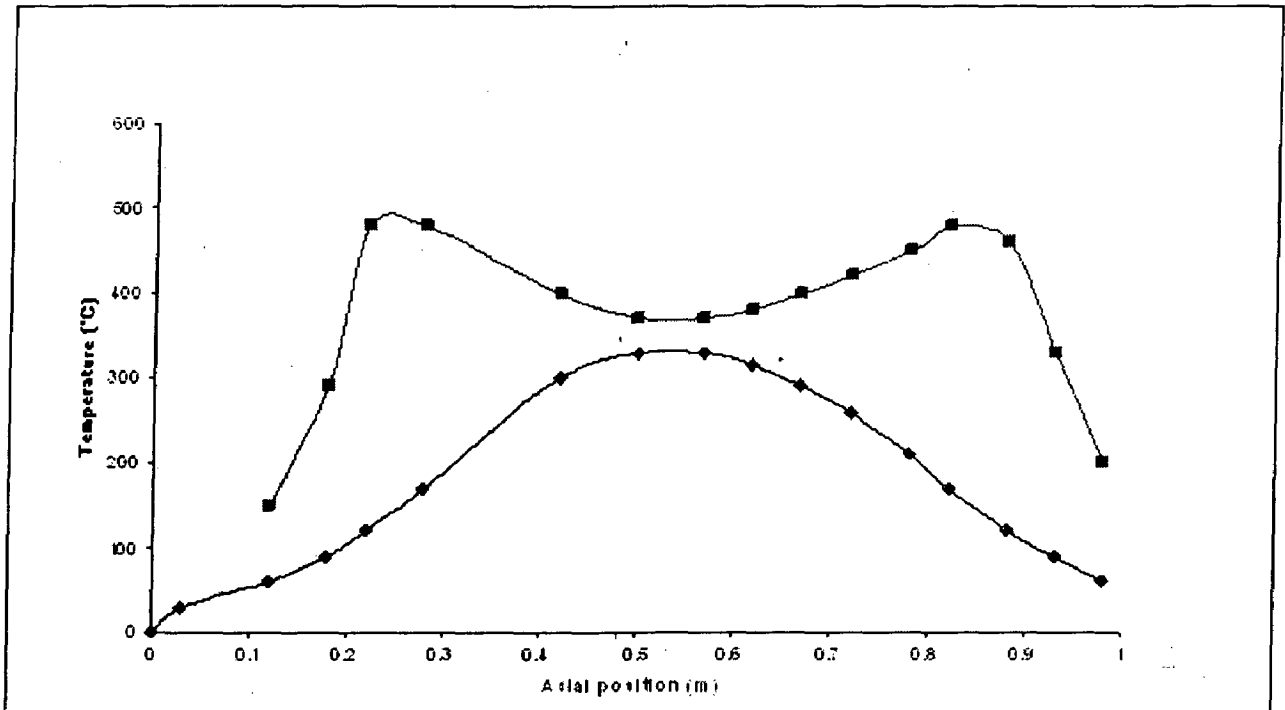


Figure 2.3: Experimental axial temperature profiles for two different concentrations.

Fig. 2.3 shows the completely different temperature profiles for two different adiabatic temperature rise of ethane. The ethane conversion is very high for higher adiabatic temperature rise whereas combustion is not complete for the lower value, which is very near to the minimum adiabatic temperature rise.

The upper curve in Fig. 2.3 is the standard profile found in a RFR for $\Delta T_{ad} > \Delta T_{ad,min}$. Now top temperature has been shifted from the centre to the inlet and outlet part of the reactor. If the reactor were truly adiabatic, the shape of the temperature profile would be plateau-like. However, radial heat losses inevitably occur, and as a result, a shallow valley appears in the middle of reactor.

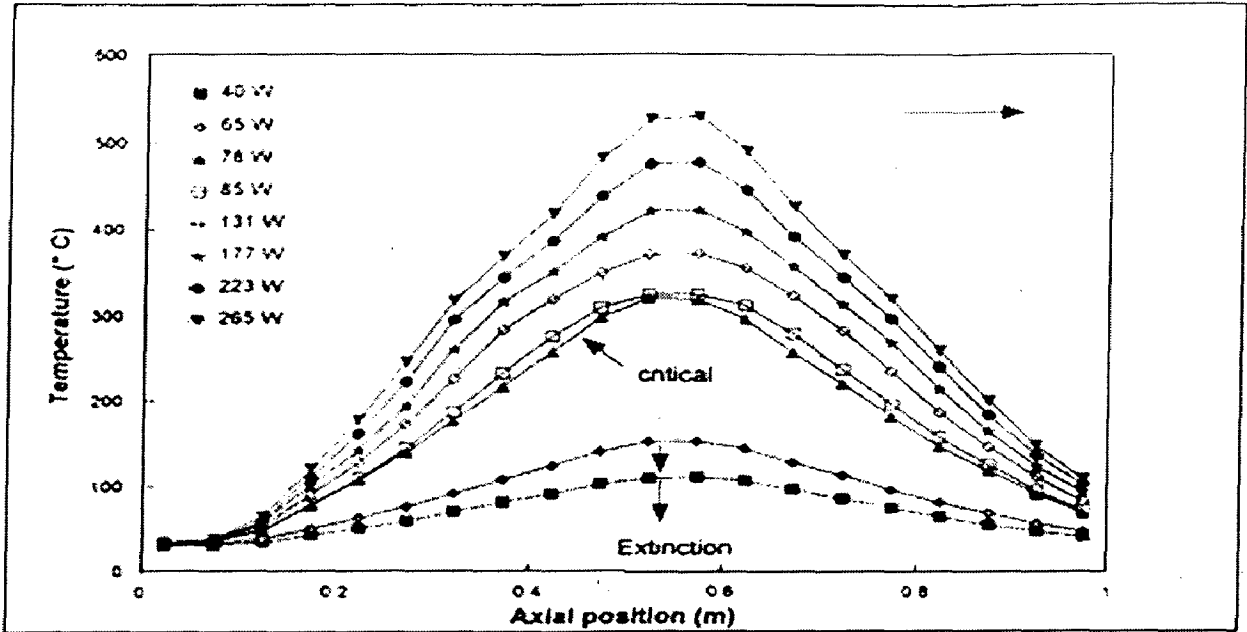


Figure 2.4: Influence of the electrical power input on the axial temperature profiles for $C_{\text{ethane}} = 0.0244 \text{ vol\%}$ or $T_r = 11^\circ\text{C}$

Fig. 2.4 shows the experimental temperature profiles for different power inputs by the internal electrical heater for the $C_{\text{ethane}} = 0.0244 \text{ vol\%}$. The adiabatic temperature rise for this concentration is 11°C , a value well below the critical value of about 21°C (van de Beld *et al.* 1994). Thus without extra energy, input reaction is extinguished. Under adiabatic conditions the heat released by the electrical heater produces a temperature rise given by the following equation

$$\Delta T_{el} = \frac{4P_{el}}{\pi_{u_0} (\rho C_p)_{g_0} D_t^2} \quad (2.3)$$

On addition of ΔT_{el} to the temperature rise due to reaction ΔT_r , we have the total adiabatic temperature rise for system as ΔT_t , which should be always greater than $\Delta T_{ad, \min}$ the reactor was operated successfully, and high conversions of the contaminants were obtained using internal electrical heater f/r lean mixtures, which require an additional heat supply for the ignited state.

The reactor has been operated successfully, and high conversions of the contaminants have been obtained using internal electrical heater for the lean mixture. Results show that for lean mixtures and a given electrical power supply the width of the electrical heater reduces the maximum temperature.

2.3 Westerterp *et al.* (1994)

The catalytic oxidation of organic contaminants in a packed bed reactor

To control air pollution, catalytic combustion can be applied to eliminate polluting volatile organic compounds. Comparing catalytic combustion to thermal combustion, heterogeneous catalysed reactions proceed at much lower temperatures. In the case of aromatic hydrocarbons, the reaction rate of one component will be influenced by the presence of other aromatic species. If the conversion of the contaminants is followed as a function of catalyst temperature, an S curve of the conversion versus the reaction temperature is to be expected. The exact shape of the curve depends on the kinetics of the reaction, mass transport, and the operating conditions of the reactor. If this curve can be described well, a tool will have to be obtained to determine the minimum reaction temperature for the 99% conversion of the compound at the specified flow rate. Of course, the minimum reaction temperature, T_{99} , can be determined directly from the experimental result. By fitting these results to a reactor model, numerical values for the kinetic parameter can be obtained.

The main assumptions in the development of the model equations are

- Condition of the reactor bed is isothermal, i.e. there are neither radial nor axial temperature gradients.
- The gas is in plug flow and it behaves ideally.
- The temperature dependence of the reaction can be described by an Arrhenius expression.
- The reactions are of the first order with respect to the hydrocarbon; oxygen is in such large excess that it does not influence the reaction rate. For all experiments the oxygen partial pressure was kept constant.
- The mass capacity of the catalyst can be neglected and the development of the concentration profiles is instantaneous; adsorption phenomena do not play an important role.
- Inter particle mass transport limitation can be neglected.

First order reaction kinetics has been assumed with respect to hydrocarbon. This means that T_{99} is insensitive to a change in inlet concentration. T_{99} was plotted as a function of the inlet concentration of ethene and ethane, respectively. For both components T_{99} increased with increasing inlet concentration which suggested a reaction order lower than one.

T_{99} was also plotted as a function of the residence time for both propane and propene. Increasing residence time resulted in decreasing T_{99} values. Shorter residence times have to be compensated for higher temperature. The conversion-temperature relation was plotted for propane and propene. The sensitivity of the propene oxidation to the reaction temperature is high, and therefore high activation energy must be expected. In general, propane and propene are representative for the alkanes and alkenes, respectively.

The conversion of propane was plotted as a function of bed temperature for different inlet concentrations of the water vapor. In general, the temperature at which the reaction starts, increases with increasing water vapor content in the feed. However, T_{99} does not change at higher temperatures; the conversion is almost independent of water concentration.

The performance of different catalysts and support material was tested. The activity of the support material was negligible. For the oxidation of alkanes, Pt was the most active. Alkenes were easily oxidized on Pd and the activity of Pt for these components was low.

A fast method was presented for the determination of minimum reaction temperature to achieve high conversions for the catalytic oxidation of hydrocarbon. The performance of different catalyst support materials was tested. The activity of support material was negligible. For the oxidation of alkenes, Platinum was the most active. Alkanes were easier to oxidize on palladium and the activity of platinum for these components was low. In general, alkenes are easier to oxidize than alkanes.

2.4 Guillermo *et al* (2002)

The spherical reverse flow reactor

In this study, a packed bed reactor made up of two hemispheres separated by an orifice plate can be operated as an adiabatic reverse flow reactor with nearly spherical symmetry.

The reactor requires little or no insulation with external temperatures limited to the adiabatic temperature rise, but much higher internal temperatures

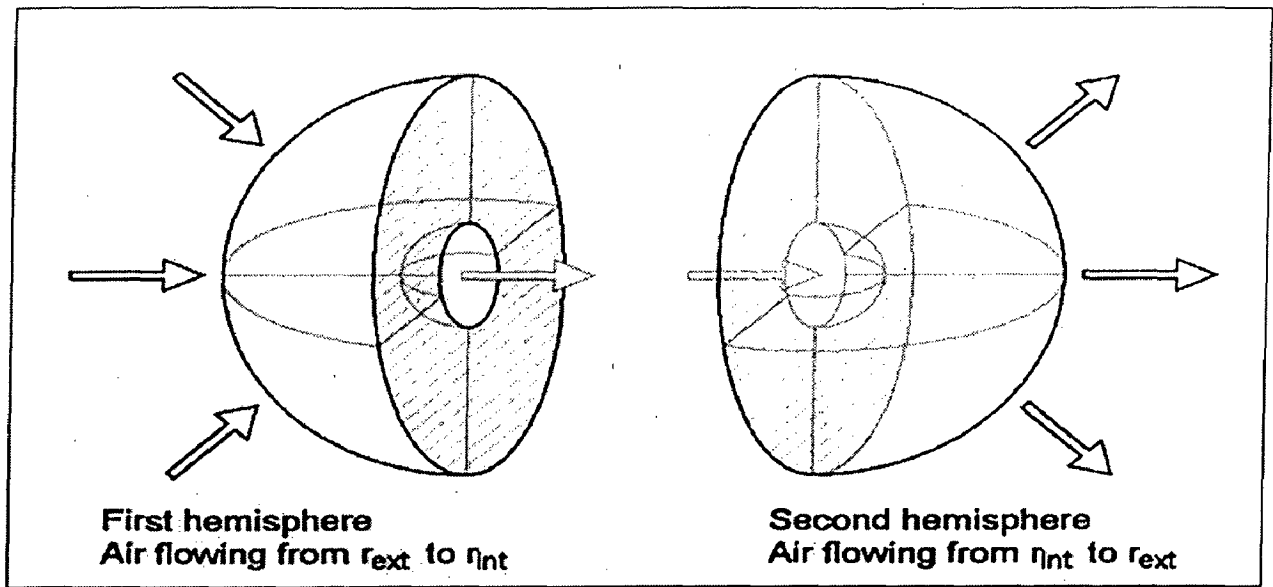


Figure 2.5: Scheme of the spherical RFR model.

In the spherical reverse flow reactor, the gas feed enters through one hemisphere and leaves through the other. Since the flow enters the reactor through the whole hemisphere, a true spherical reactor has no area where the hot region of the reactor is exposed to the surroundings. Another characteristic of the spherical RFR is that since heat transfer will be dominated by the spherical geometry, a small hot zone where reaction occurs should develop. This small reaction zone can provide several advantages, especially in reversible exothermic reactions. The target of this study is to determine the influence of the main operational and design parameters and the potential applications for this novel type of reactor. Large scale (industrial) reverse-flow reactors are nearly adiabatic and due to the tight energy budget it is important to achieve adiabatic conditions in laboratory scale. To obtain a reasonable resistance against heat losses, the amount of insulation needed is very large.

The mathematical model corresponding to the spherical reverse flow reactor (SRFR) is derived by starting from the dynamic model developed by Haynes *et al.* (1995) for tubular reverse flow reactors, making the corresponding changes for a spherical geometry.

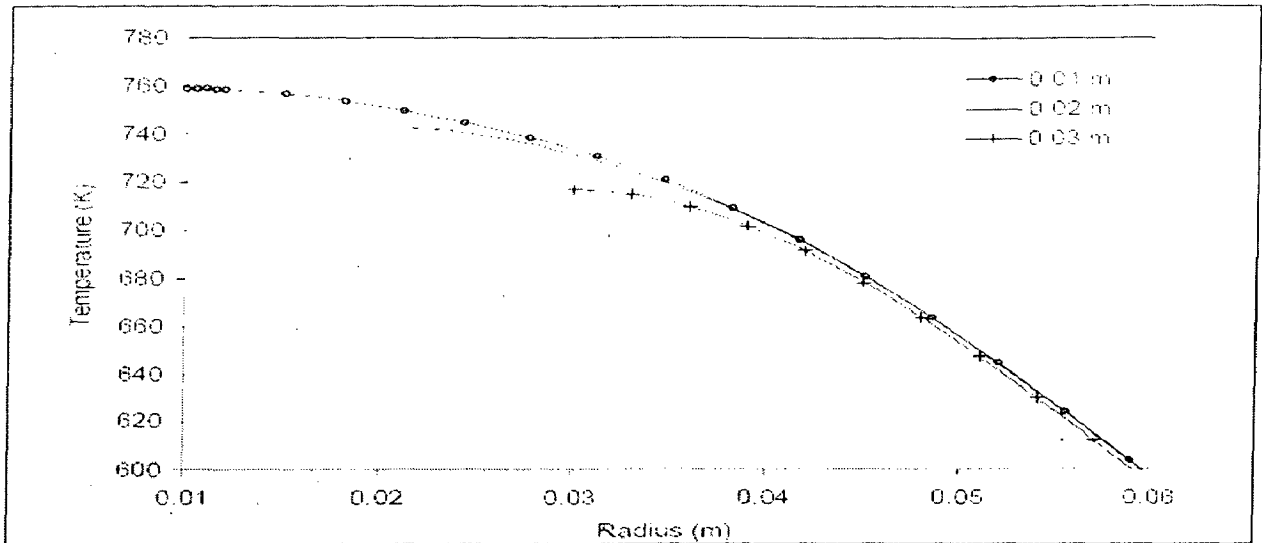


Figure 2.6: Close up of the temperature profile for different interior radius. The external radius for the three cases is 0.15 m.

Fig. 2.6 shows the temperature profiles for the high temperature region for different interior radii. It can be seen that the temperature profiles at a radius greater than 0.05 m is almost identical for the three different radii, indicating that the decrease in the interior radius has a negligible effect in the outer regions of the reactor and in the location of the reaction region, as can be verified by the conversion profiles. Therefore, decreasing the interior radius yields in a higher maximum temperature and exit conversion, due to the extra reaction volume added at high temperature.

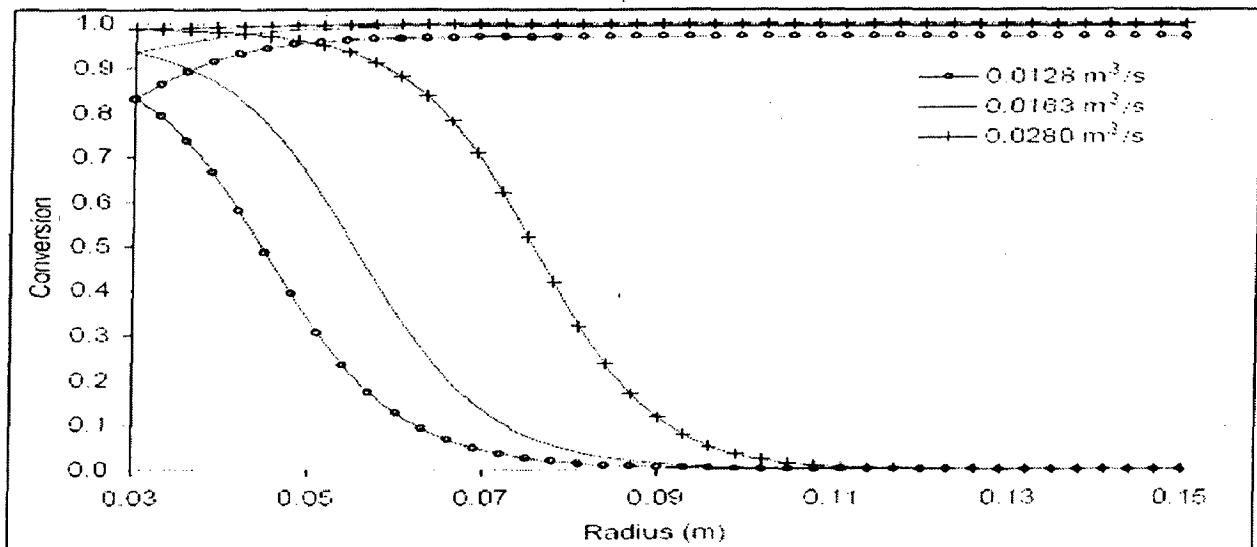


Figure 2.7: Effect of the flow rate on the conversion profiles

A conventional steady state reactor yields higher conversions at higher residence times. However, in order to obtain higher conversions in a spherical RFR, the residence time must be decreased. Fig. 2.7 shows the conversion profiles for different residence times, where the increase in conversion and decrease in residence time. The spherical RFR is shown to have an unexpectedly complex behavior. A general comparison between the spherical and the tubular RFR is difficult since the tubular RFR can be designed with different aspect ratios.

The spherical RFR was found to use a small fraction of its volume to carry out the reaction. Although the reaction region is also very small in the tubular RFR, a greater fraction of catalyst must be used due to the movement of the heat wave across the reactor. The slow down of the temperature wave helps to trap the reaction zone inside the spherical RFR, while in the tubular RFR the reaction front propagates at a constant velocity through the system requiring an additional reactor length according to the cycle time used. For the same set of parameters, the spherical RFR presents higher maximum temperature than the tubular RFR, and slightly lower conversions. The maximum temperature in the spherical RFR can be decreased by increasing the flow rate, and by increasing the cycle duration. This is not possible in a tubular RFR, since increasing the velocity increases the maximum temperature of the reactor and long cycle times do not affect the maximum temperature.

2.5 van Sint and Nijssen (2002)

A novel reverse flow reactor coupling endothermic and exothermic reactions: an experimental study

A new reactor concept has been studied for highly endothermic heterogeneously catalyzed gas phase reactions at high temperatures with rapid but reversible catalyst deactivation. The reactor concept aims to achieve an indirect coupling of energy necessary for endothermic reactions and energy released by exothermic reactions, without mixing of the endothermic and exothermic reactants, in closed-loop reverse flow operation. In a small laboratory scale reactor the concept of this 'reaction coupling reverse flow reactor' (RCRFR) has been investigated experimentally for the propane dehydrogenation coupled with methane combustion over a monolithic catalyst. However, it was necessary to reduce

the oxygen concentration during the methane combustion steps in order to avoid too high temperatures due to local combustion of carbonaceous products in the wash coat deposited during the preceding propane dehydrogenation reaction step.

The reactor concept effectuates an indirect coupling between energy necessary for the endothermic reactions and energy released by exothermic reactions using the catalyst material as an intermediary energy store. During the endothermic reaction step energy is withdrawn from the catalyst cooling down the catalyst, while simultaneously the catalyst is deactivated. During a consecutive exothermic reaction step the catalyst is reheated and concurrently regenerated. Furthermore, the direction of the gas flow through the fixed catalyst bed is periodically reversed while the reactants are fed without any preheating, which allows integration of recuperative heat exchange inside the reactor.

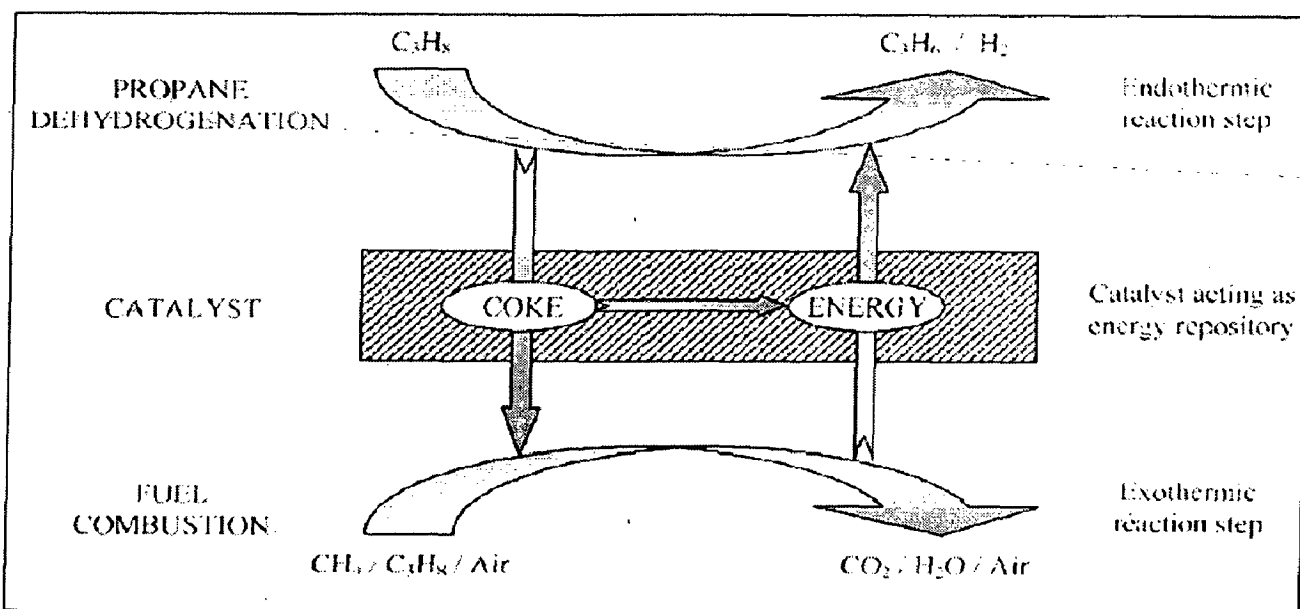


Figure 2.8: Schematic representation of the reaction coupling reverse flow reactor (RCRFR) concept for the catalytic non-oxidative propane dehydrogenation.

Application of this reactor concept, here referred to as the 'reaction coupling reverse flow reactor' (RCRFR), is especially interesting for the non-oxidative propane dehydrogenation indirectly coupled with fuel combustion over a platinum-based monolithic catalyst, schematically depicted in Fig. 2.8.

Propane dehydrogenation coupled with methane combustion over a monolithic catalyst in reverse flow has been experimentally investigated. It was shown that the absence of radial mixing in the monolithic catalyst helped minimizing radial heat losses. Despite the inevitably large influences of radial heat losses on the axial temperature

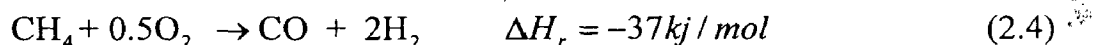
profiles the experiments have shown that endothermic and exothermic reactions can be coupled in reverse flow, integrating *in-situ* heat supply and catalyst regeneration with recuperative heat exchange. Too high temperatures in the catalyst during the methane combustion step due to local combustion of carbonaceous products deposited in the wash coat during the propane dehydrogenation cycle could be avoided by decreasing the oxygen concentration.

Propane dehydrogenation experiments in a reactor entirely filled with active catalyst showed that almost all the propylene formed at the high temperature plateau was again hydrogenated at the reactor ends, resulting in a low propane conversion. Remarkably, for higher endothermic gas velocities the propane conversion increased.

2.6 Neumann and Veser (2004)

Catalytic Partial Oxidation of Methane in a High-Temperature Reverse-Flow Reactor

The production of hydrogen and synthesis gas from methane is a key technology for the twenty-first century which is predominantly performed by steam reforming of methane. An alternative reaction route is the direct catalytic partial oxidation of methane (CPOM) at high-temperature, short contact time conditions, which proceeds auto thermally over noble metal catalysts. In this process, methane is converted with oxygen or air over noble metal catalysts to synthesis gas in a simple, one-step reaction



Thus, in principle, the process has several advantages over steam reforming of methane. The exothermicity of the reaction allows auto thermal reactor operation; that is, it renders expensive external heating unnecessary. Furthermore, the very high reaction rates permits unusually compact reactors.

The catalytic partial oxidation of methane (CPOM) processes, therefore, seems ideally suited to enable a more efficient use of methane and natural gas resources, especially in remote locations or for small-scale, decentralized and for mobile applications. The stoichiometric point for partial oxidation is at a CH_4/O_2 ratio of 2.0 and

for total oxidation at 0.5. This makes the CH_4/O_2 ratio of the feed gas a decisive parameter for influencing reaction selectivities.

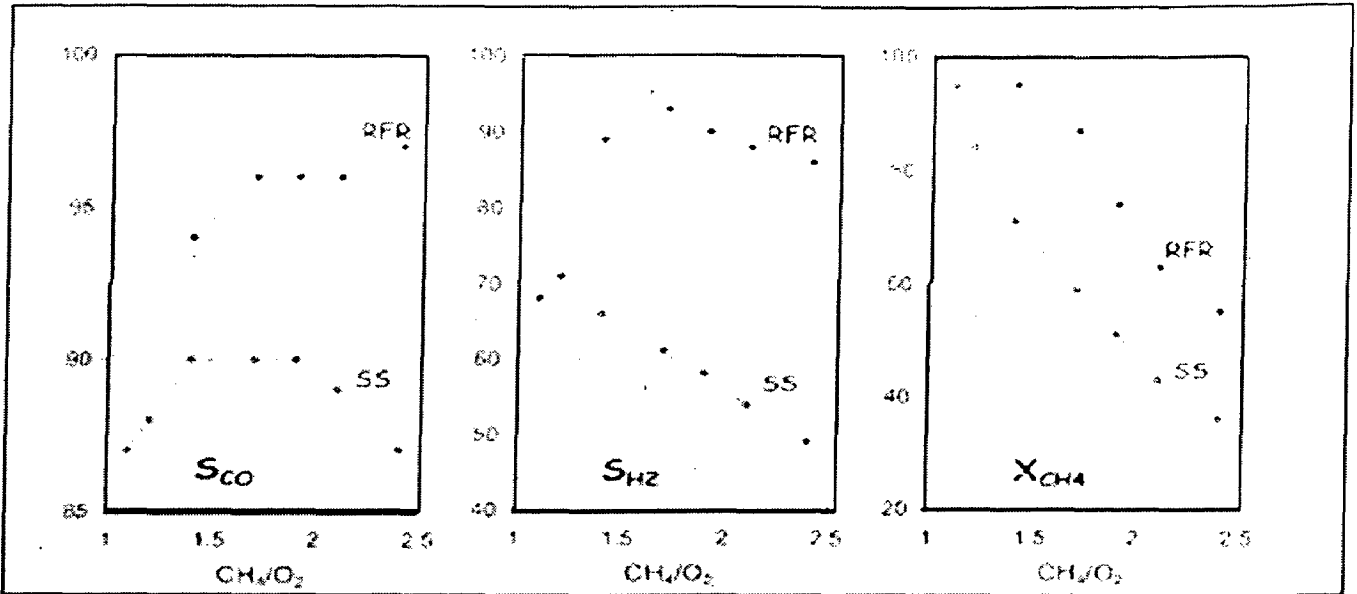


Figure 2.9: CO selectivities (S_{CO} , left), H_2 selectivities (S_{H_2} , middle), and CH_4 conversions (X_{CH_4} , right) as a function of the CH_4/O_2 ratio for steady-state (SS, dotted lines) and RFR (solid lines) operation.

Figure 2.9 show partial oxidation selectivities and methane conversions for different CH_4/O_2 ratios in the RFR in comparison to conventional steady-state (SS) reactor operation.

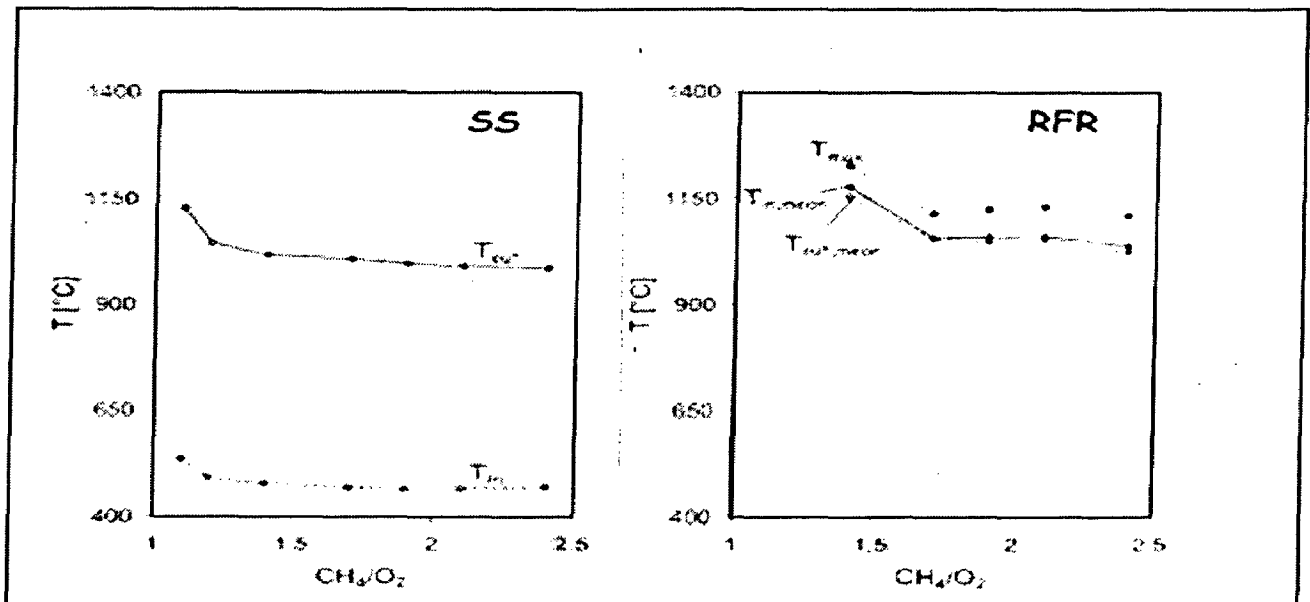


Figure 2.10: Temperatures as a function of the CH_4/O_2 ratio

The integrated heat exchange in the RFR results in increased catalyst temperatures when compared to a process without heat integration, as seen for higher temperatures in Figure 2.10. This temperature increase is particularly pronounced at the catalyst front edge. The strongly increased feed gas temperatures effectively reduce total oxidation of methane at the catalyst entrance and result in the observed pronounced increase in synthesis gas yields compared to those of conventional reactor operation. The semi cycling period $\tau/2$ is a unique operating parameter of the dynamic reverse-flow reactor. It sets the time frame during which heat is stored and removed in the inert zones on both sides of the catalyst bed, and thus has a decisive influence on temperature profiles along the reactor axis. Two limiting cases can be distinguished a priori (1) $\tau/2 \rightarrow \infty$ (that is, infinitely slow flow reversal), which corresponds to a transition to the conventional steady-state process without heat integration; and (2) $\tau/2 \rightarrow 0$ (that is, infinitely fast flow reversal), where the gas-flow stagnates and the reaction extinguishes. Thus, an optimum cycling time must exist between these two extremes.

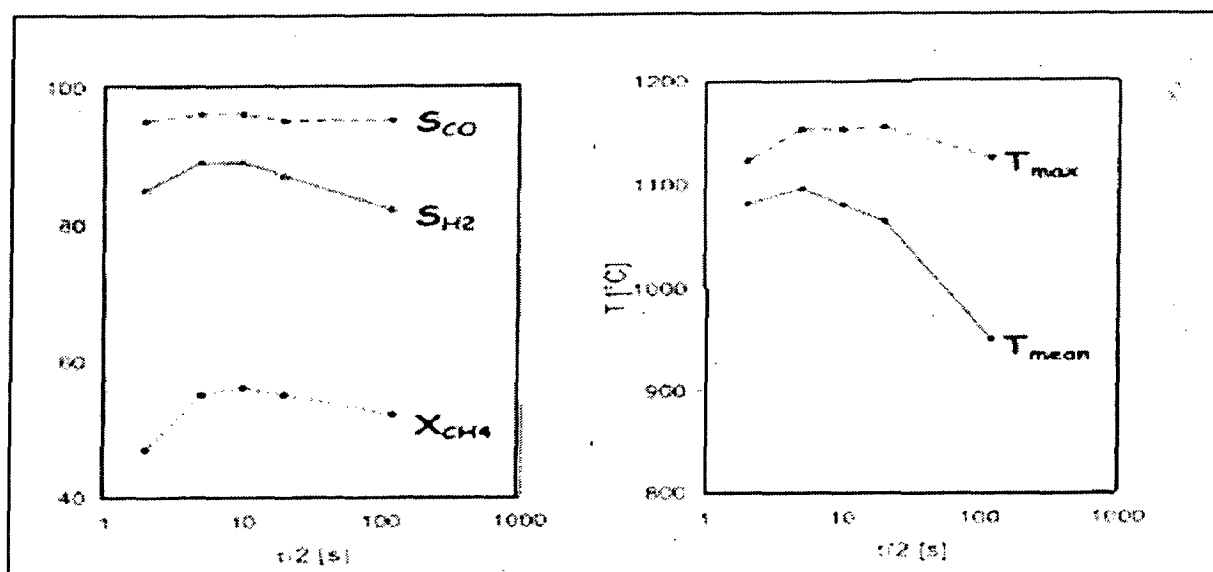


Figure 2.11: CO selectivities (S_{CO} , dashed line), H_2 selectivities (S_{H_2} , solid line), and CH_4 conversions (X_{CH_4} , dotted line, left) as well as maximum (T_{max} , dotted line) and mean temperatures (T_{mean} , solid line; right) as a function of the cycling period $\tau/2$.

Methane conversions and partial oxidation selectivities (left graph) show a maximum at a semi cycling period of about 10 s. Mean catalyst temperatures (right graph) show a maximum around $\tau/2 = 5-10$ s ($T = 1100^\circ\text{C}$), whereas maximum temperatures show a

broad maximum centered around $\tau/2 = 10$ s and vary only within 30°C over the whole range of cycling periods investigated ($T = 1120\text{--}1150^\circ\text{C}$).

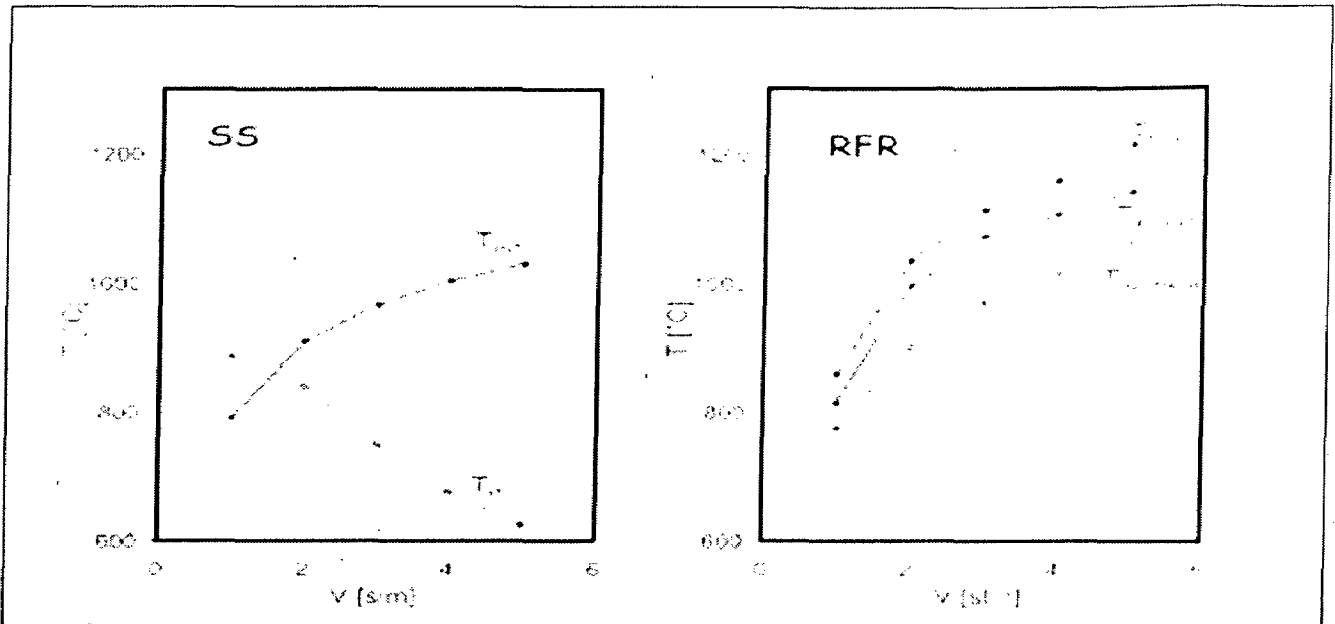


Figure 2.12: Catalyst temperatures as-a function of the total volumetric gas flow V . Left: steady-state (SS) reactor (T_{out} : solid line; T_{in} : dashed line), right: RFR (T_{max} : dashed line; T_{in} : mean: solid line; T_{out} : mean: dotted line)

Figure 2.12 shows that in the conventional process, an increase in throughput leads to decreasing catalyst entrance and increasing catalyst exit temperatures, resulting in a scissor like shape of these two temperature curves. In RFR operation, mean and maximum temperatures increase continuously with higher flow rates and run parallel to catalyst exit temperatures of the steady-state process.

2.7 van Sint *et al* (2001)

Safety analysis of switching between reductive and oxidative conditions in a reaction coupling reverse flow reactor

The strongly endothermic propane dehydrogenation is carried out at high temperatures ($550 - 650^\circ\text{C}$) because of thermodynamic constraints on the propane conversion. However, at these temperatures carbonaceous side-products, collectively termed coke, are formed at the catalyst surface, necessitating catalyst regeneration. During the endothermic propane dehydrogenation reaction phase, energy is withdrawn from the catalyst cooling down the catalyst and simultaneously coke is deposited on the catalyst surface. During

consecutive exothermic fuel combustion reaction phase, the catalyst is reheated and concurrently regenerated by burning off the coke. Upon switching between the endothermic propane dehydrogenation reaction phase to the exothermic fuel combustion reaction phase and vice versa hydrocarbons and hydrogen come into contact with oxygen, at least for a short time. Thus, due to mixing a combustible gas mixture might be formed, possibly causing a temperature runaway (hot spot) or even an explosion.

Potential hazards can obviously be avoided by flushing the reactor with inert gases like nitrogen prior to reaction phase switching. However, if a flushing cycle could be prevented this would greatly enhance the feasibility of the RCRFR by avoiding additional complexity of a flushing cycle on the already very complex dynamic reactor behavior, and by avoiding extra energy losses and nitrogen costs.

The phenomena occurring in an adiabatic RCRFR (reaction coupling reverse flow reactor) upon reaction phase switching have been modeled with mass and energy balances for the gas and catalyst phase, using a one-dimensional plug flow model with superimposed axial dispersion.

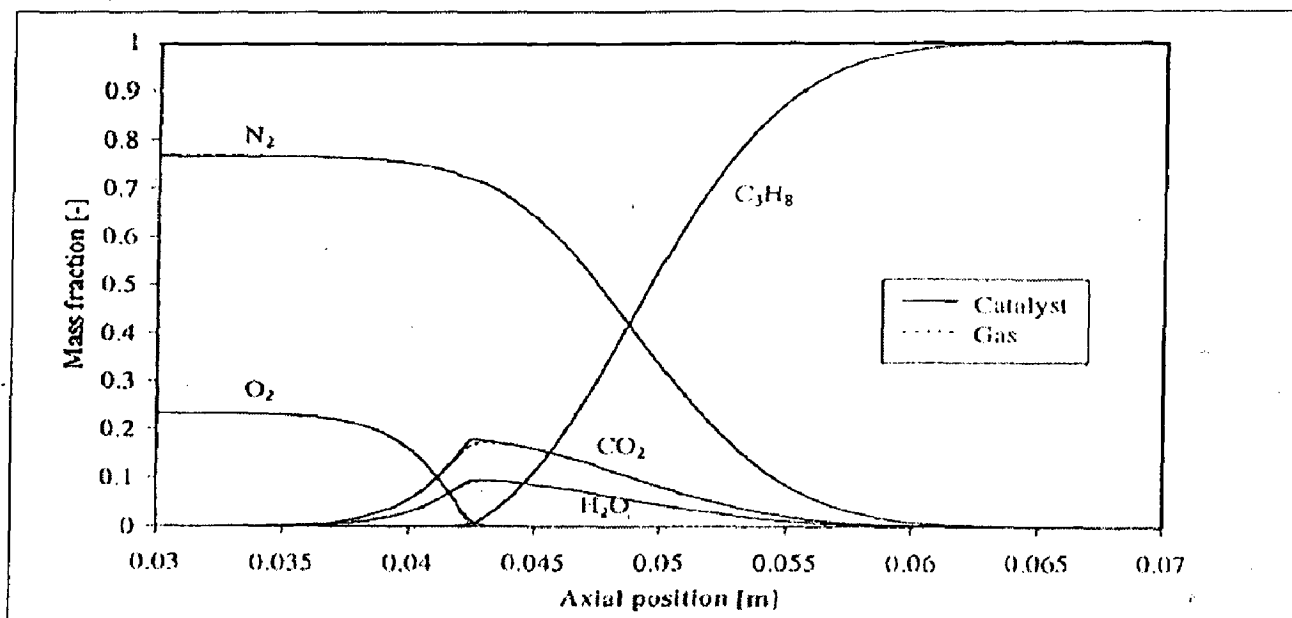


Figure 2.13: Axial mass fraction profiles after 0.05 sec. for the catalyst and gas phase in case of propane superseded with air without premixing in the inlet section

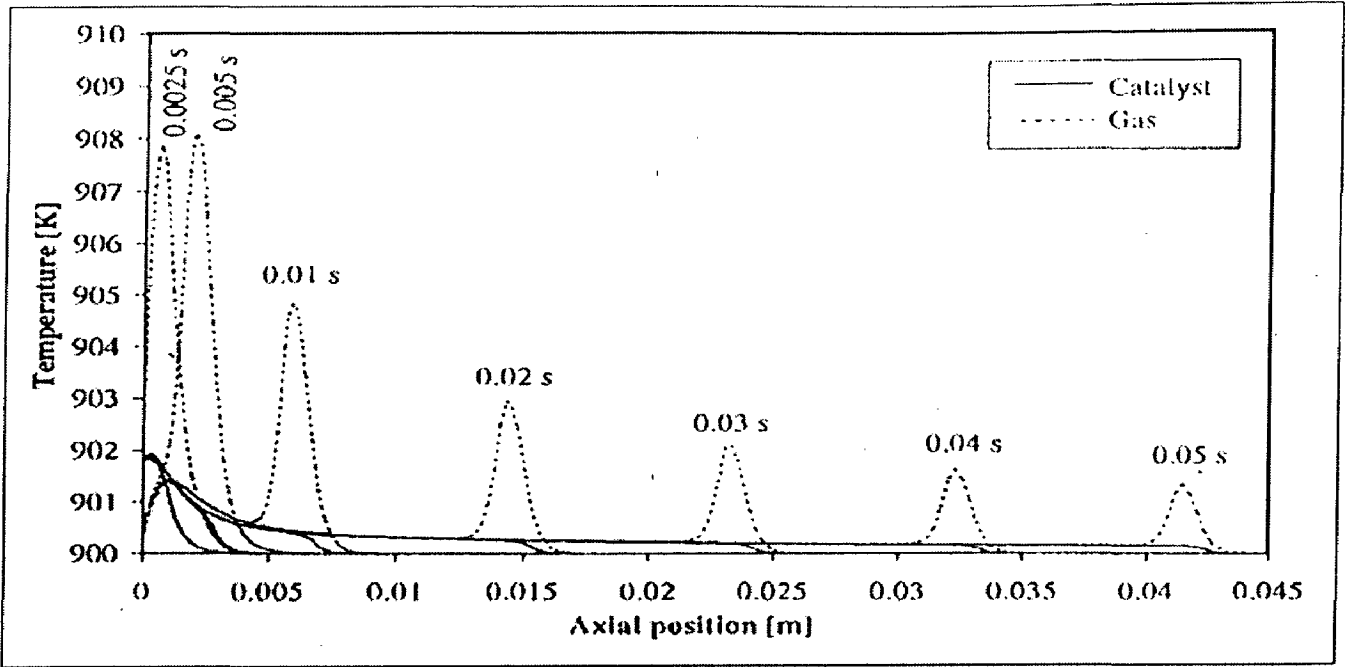


Figure 2.14: Temperature profile for the catalyst and gas phase in case of propane superseded with air without premixing in the inlet section.

Typical axial mass fraction and temperature profiles have been shown in Figure 2.14. The propane combustion reaction products accumulate between the propane and oxygen reactants, thus creating a diffusive barrier. Already after very short times the propane combustion rate becomes limited by axial dispersion of propane and oxygen.

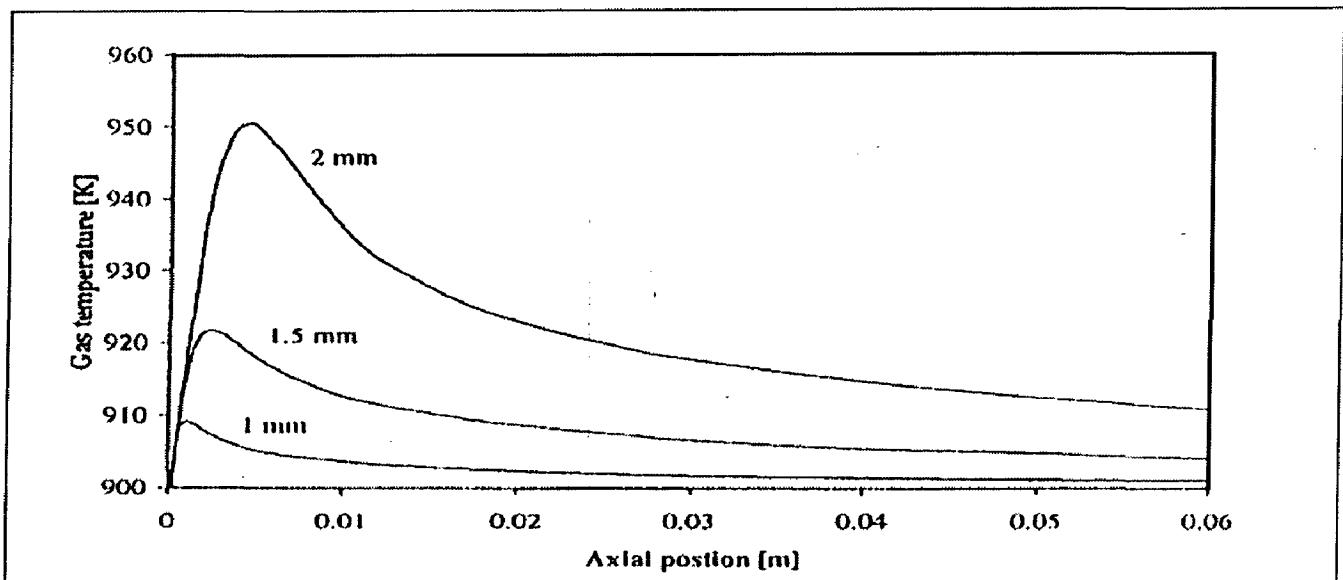


Figure 2.15: Effect of the channel diameter on the maximum gas temperature with no premixing in the inlet section

The maximum temperature rise in the gas phase strongly increases with increasing rate of axial dispersion and increasing ratio of propane conversion by homogeneous reactions as compared to heterogeneous reactions. Thus, the maximum temperature rise strongly increases for a monolith with a larger channel diameter due to the strongly increased axial dispersion.

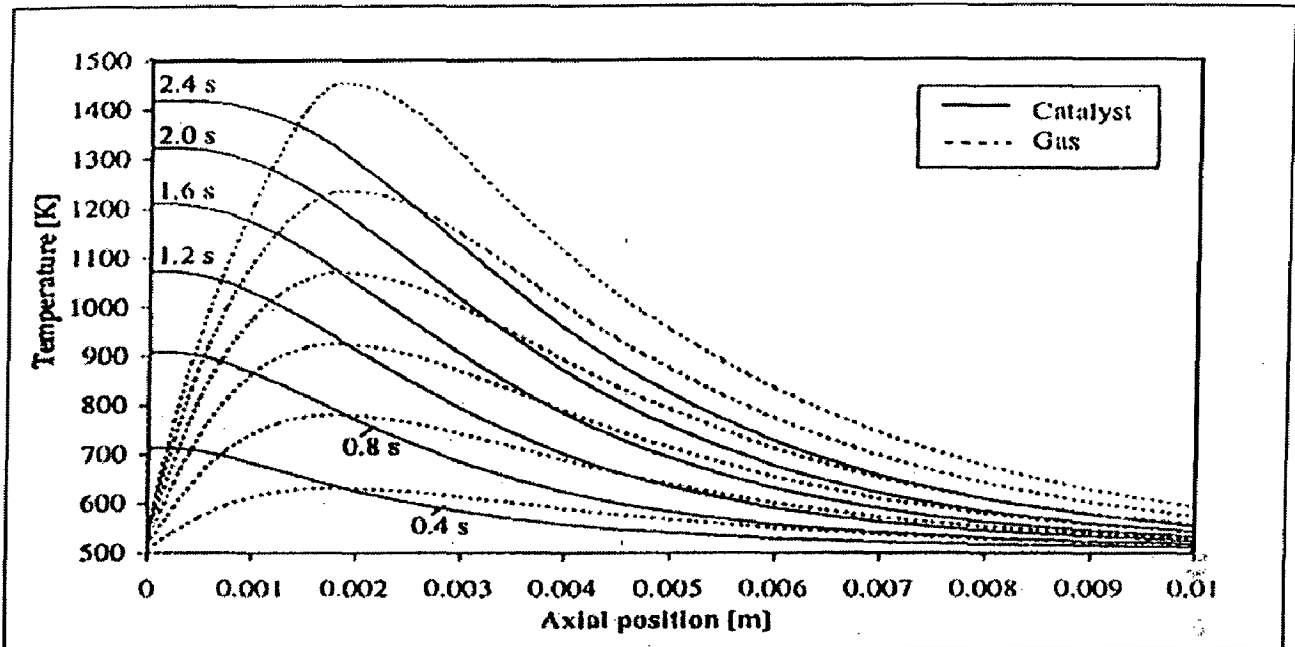


Figure 2.16: Catalyst and gas-phase axial temperature profiles at every 0.4 s when feeding a premixed propane/air mixture to a catalytic monolith.

Simulation results for the case of feeding a premixed propane/air mixture (with constant inlet composition) to a fully active monolith presented in Figure 2.16. When feeding a premixed gas mixture to a fully active monolith almost all propane conversion takes place at the catalyst surface very close to the monolith entrance, creating a hot spot in only a few seconds.

Simulations have shown that flushing with inert gases is not necessary for monoliths with a small channel diameter, if premixing in the gas inlet section is minimized and if the gas inlet and outlet temperatures are relatively low. The latter condition also excludes gas phase back-deflagrations. Due to the reverse flow concept and the high overall efficiency of the indirect energy transfer, inlet and outlet temperatures are low. The axial temperature profile further diminishes the temperature rise during reaction phase switching. To assure operation at low inlet and outlet temperatures, the monolith

inlet and outlet temperatures should be measured continuously as a safety measure. Taking proper precautions, switching between oxidative and reductive conditions can be carried out without intermediate flushing with inert gases. Without flushing, the heat released by propane combustion during reaction phase switching can actually be used to reheat the catalyst. In order to use the whole monolith effectively and obtain maximum conversion, the Damkoler numbers of the endothermic and exothermic reaction phases need to be matched. In this switching scheme the switching between the reaction phases is always carried out when the temperature front has moved somewhat further into the monolith, assuring a cold monolith inlet at a temperature equal to the gas inlet temperature (room temperature).

2.8 Mitri *et al* (2004)

Reverse flow reactor operation and catalyst deactivation during high temperature catalytic partial oxidation.

As we know that RFR operation leads to significant improvements in synthesis gas yields for CPOM (catalytic partial oxidation of methane) over a Pt catalyst. In the present study, the authors have investigated the effect of the catalyst choice on the efficiency of the reactor concept, particularly, the interplay between catalyst deactivation and heat-integration at RFR operation

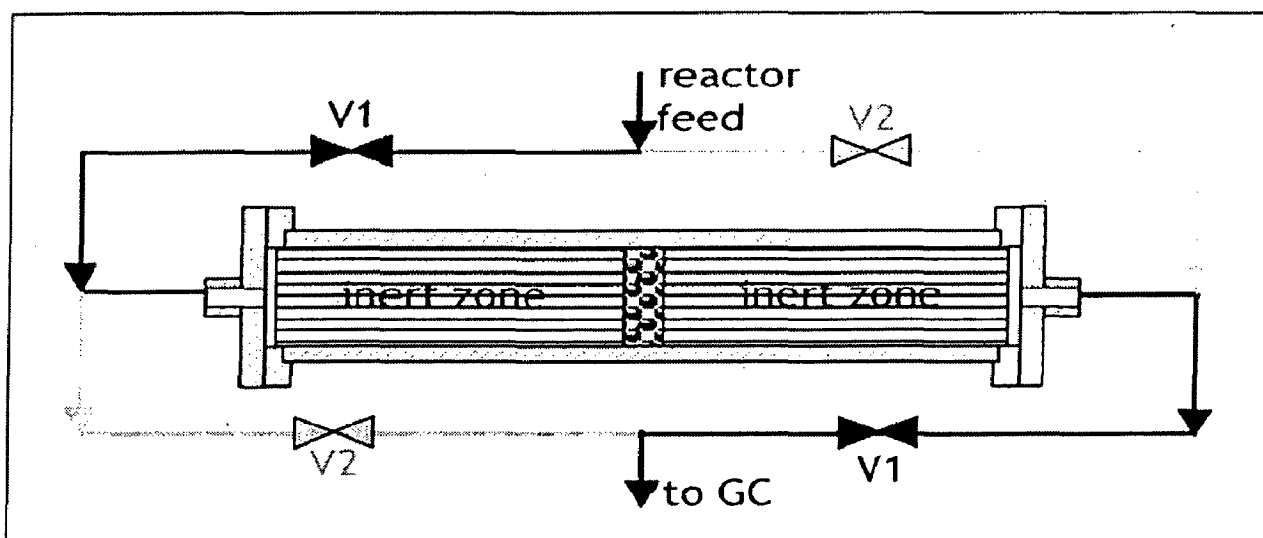


Figure 2.17: Schematic drawing of the reactor set-up. The catalyst (cat) is positioned between two inert zones. Four computer-controlled valves, which are operated in pairs (V1 and V2) allow for reversal of the flow direction in the reactor.

The objective of this study is thus to determine how robust and widely applicable this reactor concept is at typical conditions for high temperature catalytic processes.

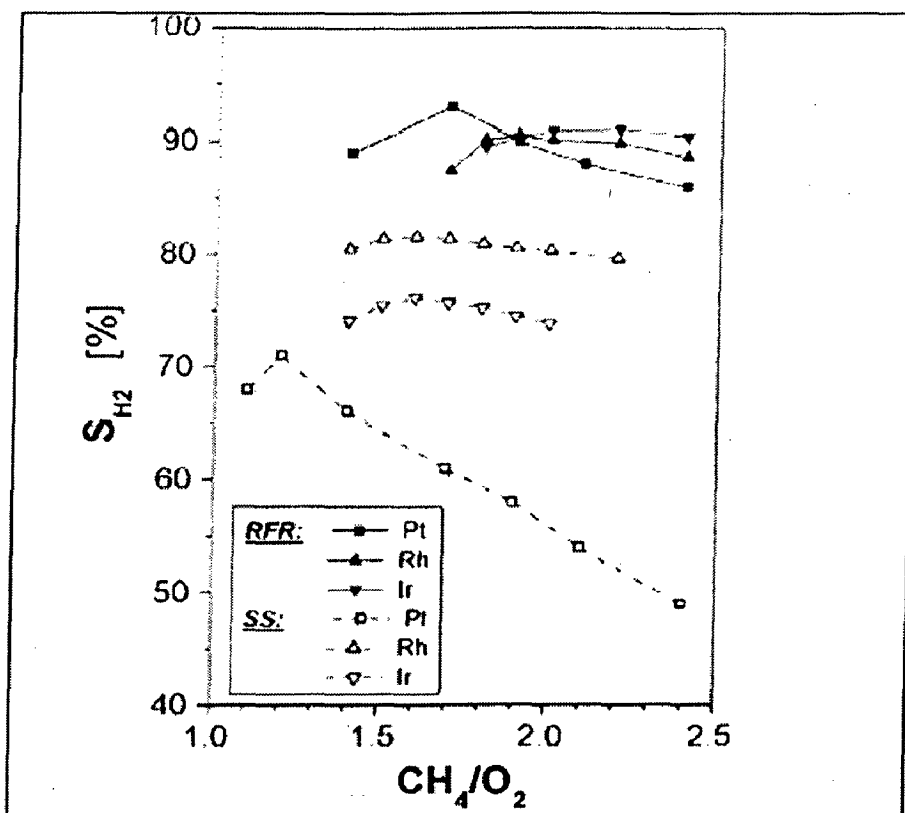


Figure 2.18: Direct comparison of hydrogen selectivities at steady state operation (open symbols and dotted lines) and reverse-flow operation (full symbols and solid lines) for Pt, Rh and Ir, showing the equalizing effect of RFR operation on catalyst performance.

Beyond the strong improvements in synthesis gas yields for each of the three catalysts, it seems particularly remarkable to note that RFR operation leads to a strong “equalizing” of catalyst performance, as shown in Figure 2.18, where hydrogen selectivities for Pt, Rh and Ir at SS and RFR are shown in direct comparison. One can see that the widely spread hydrogen selectivities at SS converge into a narrow band around 90% at RFR operation.

Obviously, reverse flow operation leads to particularly strong improvements for less active and selective catalysts and thus appears to be an elegant and efficient way to overcome catalyst short-comings through reactor engineering.

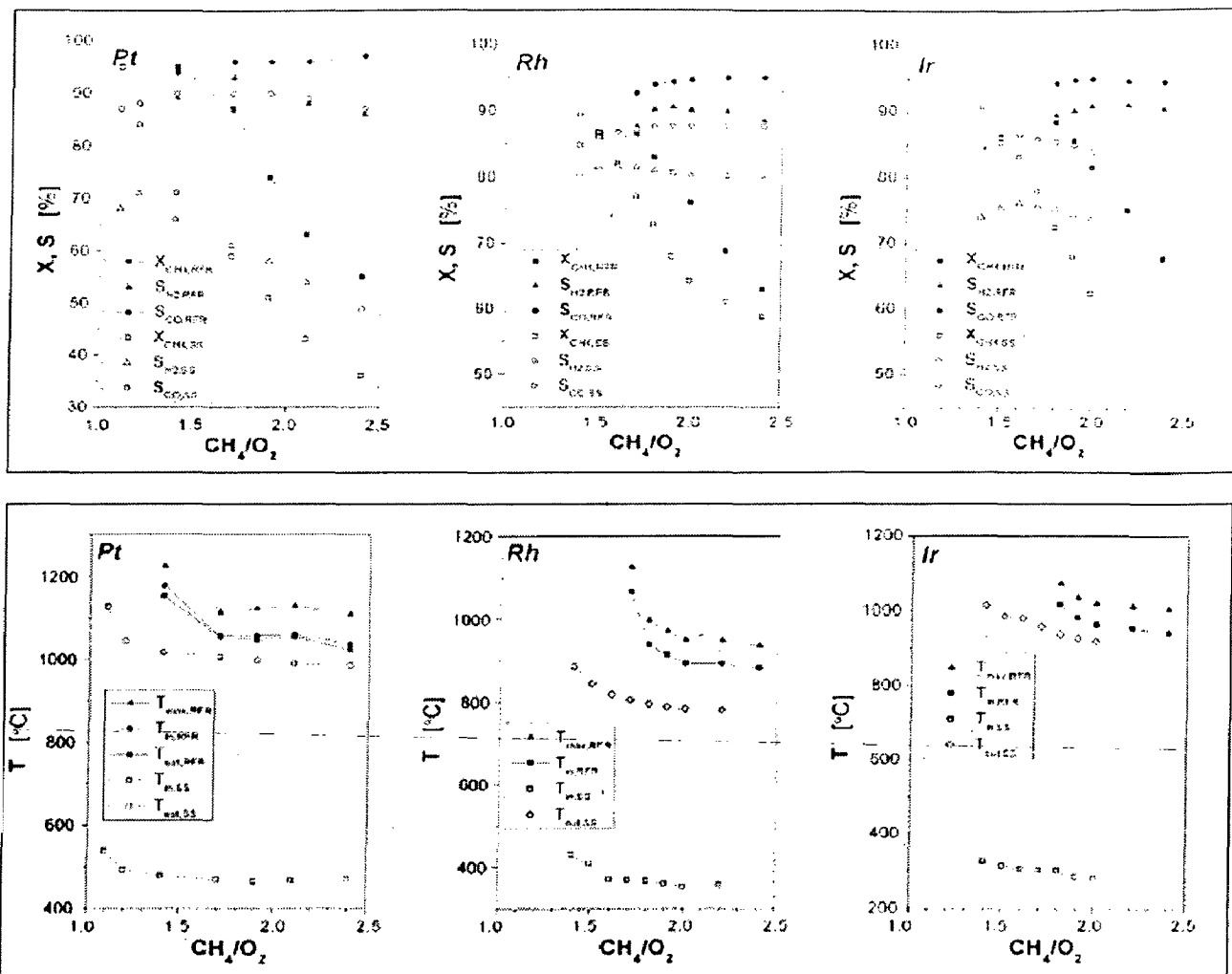


Figure 2.19: Methane conversion and syngas selectivities (upper row) and catalyst temperatures (lower row) versus total volumetric inlet flow rate at steady-state reactor operation (open symbols and dotted lines) and reverse-flow operation (closed symbols and solid lines) for the Pt catalyst (left column), Rh catalyst (middle column) and the Ir catalyst (right column). Inlet gas composition was $\text{CH}_4/\text{O}_2/\text{N}_2 = 2/1/4$ and the duration of a half period at RFR operation was 15 s.

Results have been shown in Figure 2.19, where again methane conversion and hydrogen and CO selectivities (top row) as well as catalyst temperatures (bottom row) at SS and RFR are shown for all three catalysts for volumetric inlet flow rates between 1 and 5 slm (standard liters per minute, $\approx 1.7\text{--}8.3 \cdot 10^{-5} \text{ m}^3/\text{s}$). Again, all three catalysts show very similar behavior: at the lowest flow rate, methane conversions and CO selectivities are almost identical at SS and RFR operation, and S_{H_2} is only mildly improved by RFR operation. With increasing flow rate, however, RFR operation leads to increasingly strong improvements over SS operation. It seems particularly noteworthy that, while results at SS

show a maximum between 2 and 3 slm for all three catalysts, results at RFR operation continue to improve over the whole range of experimentally tested flow rates.

The results indicate that the efficient regenerative heat integration which can be achieved in a reverse-flow reactor make this reactor concept particularly well suited for short contact-time reactions. Heat integration leads to a very efficient conversion of thermal energy to chemical energy, improving synthesis gas yields significantly for all three catalysts in this study (Pt, Rh, Ir). Since all observed effects can be traced back to the interplay between heat integration and improved yields at higher reaction temperatures, similar effects and improvements can be expected for a wide range of related partial oxidation reactions.

2.9 Jeong and Luss (2003)

Pollutant destruction in a reverse flow chromatographic reactor

A reverse flow reactor (RFR) is a packed bed reactor in which the feed flow direction is periodically reversed. When an exothermic reaction is conducted in a RFR it traps a hot zone in the reactor. This enables an efficient adiabatic operation at high temperatures even for feeds having a low adiabatic temperature rise. Moreover, the declining temperature of the trapped hot zone increases the yield of equilibrium-limited exothermic reactions. A reverse flow chromatographic reactor (RFCR) is a packed reactor in which the flow direction is reversed periodically and in which one of the reactants is strongly adsorbed on the catalyst. The study shows the performance of a RFCR used to destruct a pollutant A by a reaction with a reactant B, the emission level of which is subject to even stricter restrictions. Due to safety considerations, this reactant B is introduced in the center of the reactor. The RFCR operation enables a reduction of the regulated effluent products well below the minimum attainable under a steady-state operation of the same packed-bed reactor. Moreover, it can respond effectively to any perturbations in the pollutant feed rate and/or concentration. When the environmental regulations on the emission of B are stricter than those of A, it is often advantageous to feed slightly less B than the amount needed for complete conversion of A.

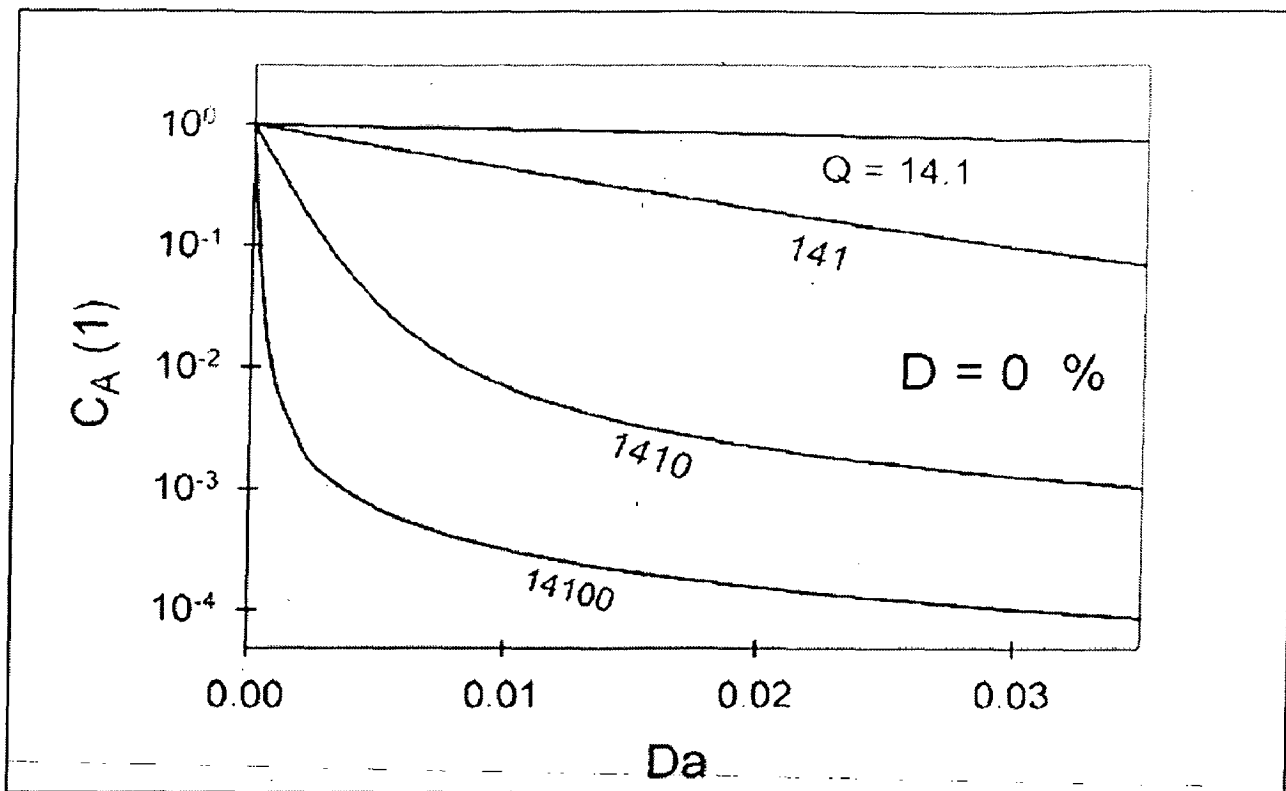


Figure 2.20: Influence of the dimensionless adsorption capacity on the steady-state pollutant effluent concentration from a packed-bed reactor.

Strong adsorption of the reactant B is advantageous also when the reaction is carried out in a packed-bed reactor. This is illustrated by Figure 2.20, which shows that increasing the dimensionless adsorption capacity of the catalyst, Q , significantly decreases the steady state pollutant effluent concentration from a packed-bed reactor to which both A and B are fed at the entrance to the reactor.

This study shows that the periodic operation of a RFCR can be much more efficient than the steady-state operation of the same chromatographic packed-bed reactor. Specifically, the RFCR operation enables a reduction of regulated effluent products well below the minimum attainable under a steady-state operation of the same packed-bed reactor. Moreover, it can respond more effectively to any perturbations in the pollutant feed rate and/or concentration. These advantages are a strong incentive to explore its application to a variety of processes involving the destruction of pollutants. At present, the only reported applications of the RFCR are for destruction of pollutants. Other creative application will probably be developed in the future

2.10 Tullilah *et al* (2003)

Flow-rate effects in flow-reversal reactors: experiments, simulations and approximations.

The advantage of reactors with periodic flow-reversal over simple once-through operation has been demonstrated in many studies of adiabatic units during the past decade. The higher temperatures attained in such units make them especially attractive for catalytic VOC oxidation or NO reduction if the temperature of the hot-zone can exceed the ignition point of the dilute reactant stream. Design and operation of a reactor with flow reversal requires accurate prediction of the domain of operating conditions, and especially the range of flow rates, where the ignited state exist. In this work the comparison of experimental observations of flow-rate effects during ethylene oxidation on Pt/Al₂O₃, with simulations of this reactor using a kinetic rate expression that was derived elsewhere and with approximate solutions based on instantaneous or very fast reactions. The oxidation of ethylene on supported Pt catalyst, that is employed here as a model reaction, is a complex reaction characterized by self-inhibition (expressed by Langmuir-Hinshelwood kinetics), by strong activation energy and by strong thermal effects that lead to a wide domain of steady-state multiplicity.

Increasing the flow rate will diminish the contact time and may eventually lead to extinction. Obviously, decreasing the flow rate will lead to declining temperature and extinction as well. It is important therefore to find and predict the domain, where the reactor with flow reversal can be operated and that is the purpose of the present contribution.

Ethylene oxidation on supported Pt catalyst is a highly activated and highly exothermic reaction and its rate is characterized by self-inhibition, leading to a wide domain of steady-state multiplicity and a strong dependence on temperature. The analysis of a flow-reversal reactor for such reactions can be approximated using the assumption of an instantaneous reaction as the feed meets the catalyst layer.

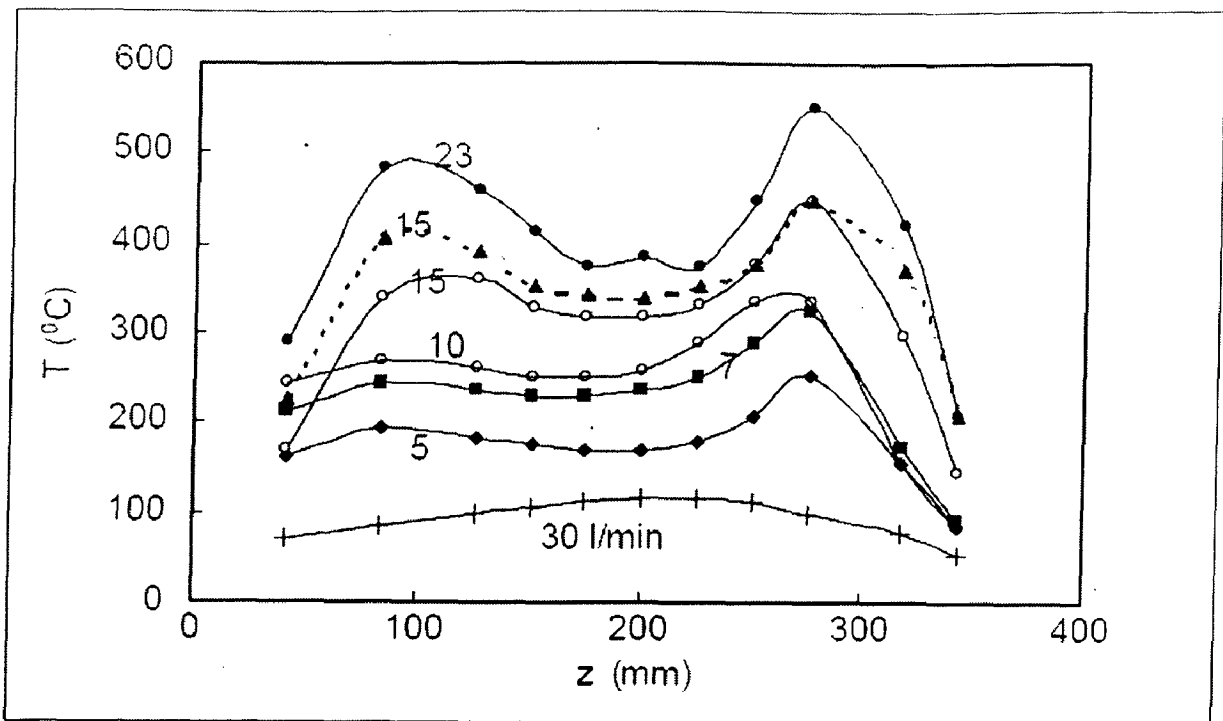


Figure 2.21: Experimental axial temperature profiles for flow reversal operation with various flow rates and feed concentration of 0.5%; extinction occurred upon increasing the flow rate to 30 l/min.

In Figure 2.21 the profile shown for 30 l/min. is a transient leading to extinction; the two profiles denoted by 15 l/min. were taken a year apart to check the reproducibility of the system.) Decreasing flow rates led to lower temperatures at the peaks and at the center with the peak positions moving to the catalytic domain and away from the entrance position.

In this work comparison of experimental observations of flow-rate effects during ethylene oxidation on Pt/Al₂O₃, with simulations approximate solutions. Adequate agreement between the experimental results and simulations, using homogeneous or heterogeneous reactor models with no adjustable parameters, is demonstrated. The difference between the homogeneous and heterogeneous model predictions is usually small.

2.11 Cittadini *et al* (2001)

Reverse flow catalytic burners: response to periodical variations in the feed

The treatment of organic gaseous emissions by combustion in catalytic reverse flow reactors has been the subject of many researches in the past years, above all because this process makes it possible to treat lean gas mixtures without the consumption of large

amounts of auxiliary fuel. Nevertheless, some practical aspects concerning the application of this technology to real industrial plants have been scarcely investigated so far. One of these is the effect of unsteady characteristics of the pollutant flow, especially for the plants where the operation schedule produces periodical variations in the inlet concentration and flow rate.

An in-depth analysis has been carried out about the behavior of a reverse flow combustor for the treatment of low-VOC concentration waste gases, in the presence of periodical variations in the feed characteristics. Two kinds of variations have been taken into consideration: in the inlet concentration and in the flow rate. In both cases, the variations cause relevant fluctuations in the maximum temperature of the bed and in conversion. These fluctuations, especially for long feeding cycle periods, can endanger the correct operation of the reactor. In addition, for particular ratios between the feeding cycle period and the flow-reversal cycle period, the interaction between the two cycles may cause serious problems of instability, represented by large low-frequency fluctuations of the maximum temperature in the case of variations in the inlet concentration, and by a dangerous flow asymmetry in the case of variations in the flow rate. In particular, the influence of the feed characteristics on the minimum inlet concentration for auto thermal operation has been evidenced. In fact, in a reactor whose main advantage is to allow the combustion of very lean mixtures, this parameter can be considered as an indicator of its performance.

The model adopted for the simulations is composed of three differential equations (one energy balance for the solid phase, one energy balance for the gas phase and one mass balance for the gas phase) and two algebraic equations (the mass balance for the solid phase and the kinetic expression). Energy accumulation in the solid and gas phases is taken into consideration, while mass accumulation is considered only in the gas phase and neglected in the solid phase. For the differential equations, conventional Danckwert's boundary conditions are assumed. The PDE system is reduced to a set of ODEs, by discretizing the spatial derivatives on a grid of evenly spaced points.

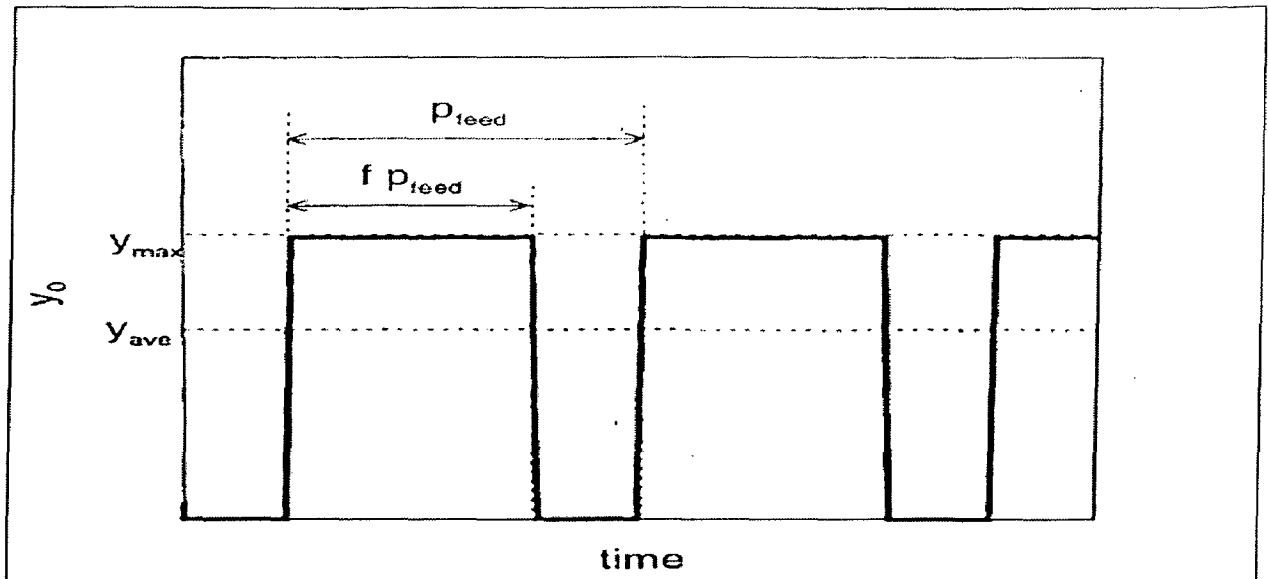


Figure 2.22: Periodical variations in the inlet concentration.

In Figure 2.22, the typology of the investigated variation is shown: square-wave fluctuations between a maximum molar fraction and zero. The parameter f represents the fraction of active feeding in the period. This behavior in the inlet concentration is present whenever the pollutant is produced in a multi step process, in which periods of production are alternated with periods of maintenance.

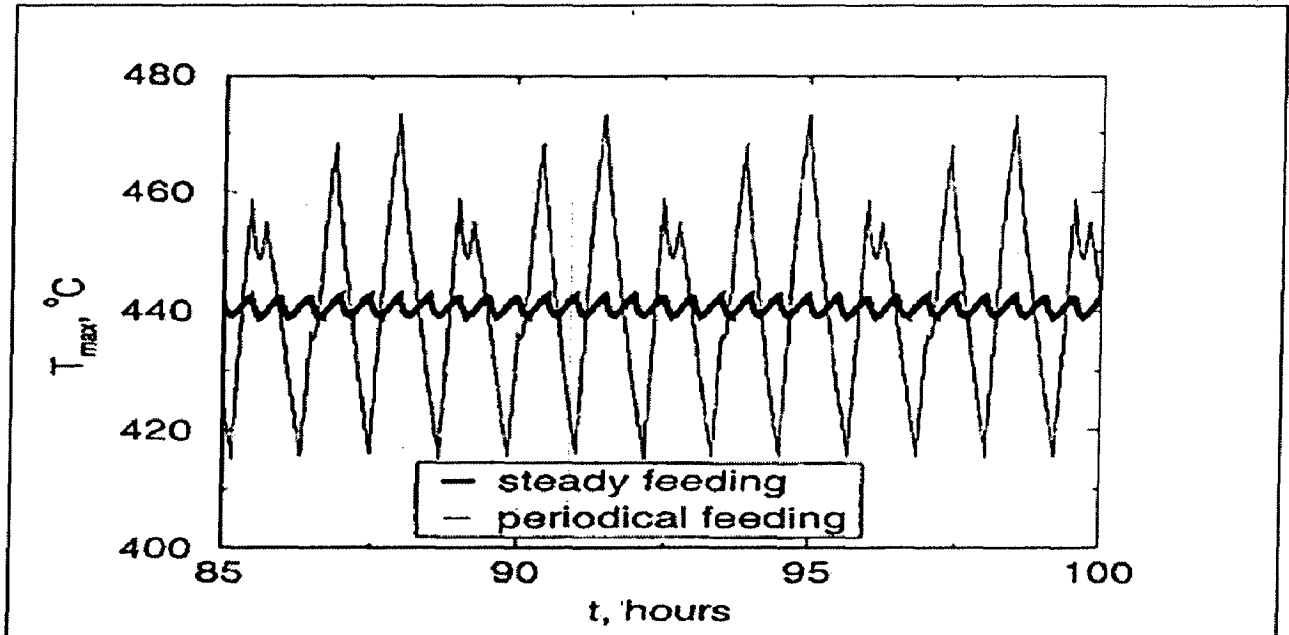


Figure 2.23: Fluctuations of the maximum temperature in the reactor, when the pseudo-steady state has been reached.

In Figure 2.23, the typical pseudo-steady-state trend of the maximum temperature in the case of constant feeding and in the case of periodical feeding are compared. In the former case, the fluctuations are very small (in the range of a few degrees) and their period is equal to the flow-reversal semi-period. In the latter case, the amplitude of the fluctuations is much larger.

The effects of periodical variations of the inlet concentration and flow rate in a reverse-flow catalytic reactor for the treatment of polluted air have been investigated. Both these kinds of disturbances produce relevant fluctuations in the maximum temperature and in the outlet concentration. In the design of the reactor, particular attention must be paid to the ratio between the feeding cycle period and the flow reversal cycle period concentration. This means that the reactor size must be chosen large enough so that a flow reversal cycle longer than the feeding cycle can be adopted. About the periodical variations in the flow rate, the main effect that has been found is related to the possibility of a difference between the average flow rate in one direction and the average flow rate in the other one.

2.12 Dufour and Touré (2004)

Multivariable model predictive control of a catalytic reverse flow reactor

This paper describes the multiple input multiple output (MIMO) model predictive control (MPC) of a catalytic reverse flow reactor (RFR). The peculiarity of this process is that the gas flow inside the reactor is periodically reversed in order to trap the heat released during the reaction. The objective of this paper is to propose a solution to avoid the limitation seen in a previous study for the single input single output (SISO) control case. It was dealing with the impossibility to avoid degradation of the catalytic elements due to the excessive heating induced by the exothermic reaction. In order to overcome this issue, a ratio of the inlet (cold) gas flow is now bypassed into the central zone. This allows introducing a second manipulated variable: the dilution rate. The phenomenological model considered here for the MIMO MPC of the RFR is obtained from a rigorous first principles modeling.

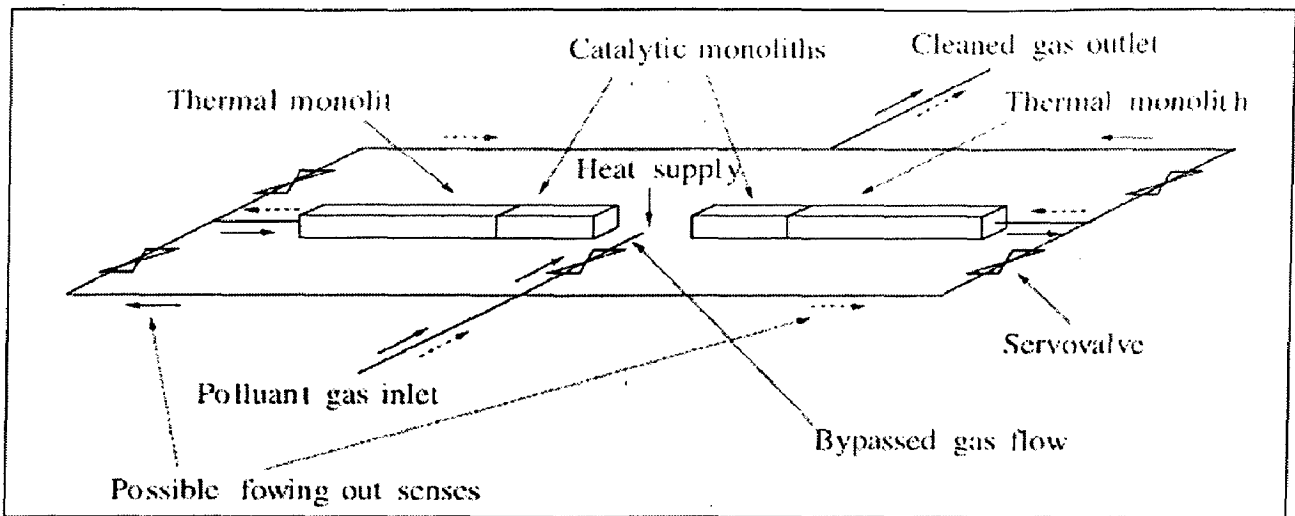


Figure 2.24: Principle scheme for the catalytic reverse flow reactor.

The operation procedure of the reverse flow reactor is described below:

A semi-cycle begins as follows: the gas flows through the first thermal monolith. It is made up of cordierite and of n_{bc} canals where the gas flows. The shape of its section is a nest. The increase of gas temperature in the canals is due to the heat exchange with the cordierite. No reaction takes place and cooling action is possible.

The gas then passes through the first catalytic monolith. This one is like the first thermal monolith but with catalytic elements (platinum and other noble metals) layers on the canals surface. With these elements, the exothermic chemical reaction takes place, inducing increase of temperature in the cordierite and a concentration of pollutant drop. A cooling action is possible.

The gas flows now in the empty central zone where two control actions are both provided: heating and cooling sources. The reaction continues in a second catalytic monolith and finally the gas reaches a second thermal monolith where no reaction occurs but where the heat of reaction is exchanged from the gas to the cordierite

At the end of this semi-cycle, the switch of the four servo valves reverses the flow rate inside the monoliths. A second semi-cycle, identical to the first one, starts but in the reverse circulation sense. Since the circulation sense has changed, the polluted gas passes first through the previous second thermal monolith. In this zone, the gas temperature increases using the heat previously accumulated in the monolith during the first semi-cycle: this is the saving mode of the process. At the end of this second semi-cycle, the

flow rate in the reactor is again reversed thanks to the servo valves switch and a new complete cycle begins.

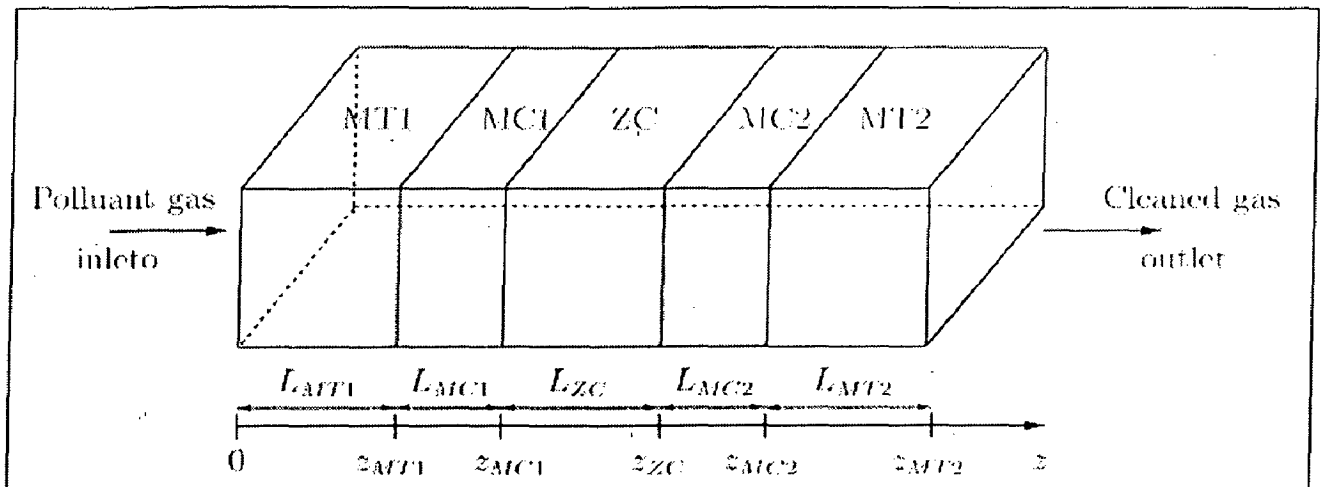


Figure 2.25: Spatial discretization in the reactor

According to the operating conditions, various problematic behaviors can take place.

An insufficiently polluted gas at the RFR inlet causes, by its low heat release during the reaction, the extinction of the reactor. With a strongly polluted gas at the RFR inlet, the release of heat due to the reaction can deteriorate the catalysts and produces thermal overheating.

To overcome extinction and overheating, several technical solutions have been proposed (Nieken, Kolios, & Eigenberger, 1995) and are used in this work.

- Extinction: fuel addition in the gas or energy addition in the central zone.
- Overheating: Use of a bypass to redirect some amount of the gas or injection of cold gas in the central zone.

This paper was dealing with the MIMO MPC of a catalytic reverse flow reactor. This process is used to decrease noxious VOC amount in gas released in the atmosphere. The complexity of this process included distributed aspect, nonlinear dynamic behavior and periodic reversing of the circulation of gas.

CHAPTER 3

MATHEMATICAL MODEL

To study the behavior of reverse flow reactor, a heterogeneous model has been developed. In order to derive the model equations, the following assumptions have been made:

- The time dependent terms in the mass balances and the gas phase heat balance can be neglected. Gawdzik and Rakowski (1988) showed this assumption does not have a significant influence on the calculated profile in the reverse flow reactor.
- The reactor pressure is constant through out the reactor.
- The gas is in plug flow, the influence of flow non-uniformities is negligible.
- Temperature and concentration gradients with in a catalyst pellets can be neglected.

The combustion kinetics of the different components is independent and is of the first order in organic compound.

Dimensional model equations

By applying mass and heat balances, Matros *et al.* derived various heterogeneous model equations in dimensional form. Later by inserting some dimensionless group, these equations are converted into dimension less form.

Heat balances:

$$\text{Gas: } 0 = -(\rho C_p)_g u_g \frac{\partial T_g}{\partial z} - \alpha_p a_p (1 - \varepsilon)(T_g - T_s) + \frac{\partial}{\partial z} \left(\varepsilon \lambda_{eff} \frac{\partial T_g}{\partial z} \right) - U_w a_w (T_g - T_w) \quad (3.1)$$

$$\text{Solid: } (1 - \varepsilon)(\rho C_p)_s \frac{\partial T_s}{\partial t} = \alpha_p a_p (1 - \varepsilon)(T_g - T_s) - \sum r_j H_j \quad (3.2)$$

$$\text{Wall: } (\rho C_p)_w \frac{\partial T_w}{\partial t} = U_w a_w (T_g - T_w) - U_\infty a_w (T_w - T_\infty) + \frac{\partial}{\partial z} \left(\lambda_w \frac{\partial T_w}{\partial z} \right) \quad (3.3)$$

Mass balance for component j:

$$\text{Gas: } 0 = -\frac{\partial u_g C_{gj}}{\partial z} - k_{gj} a_p (1 - \varepsilon)(C_{gj} - C_{sj}) + \frac{\partial}{\partial z} \left(\varepsilon D_{eff} C_i \frac{\partial y_{gj}}{\partial z} \right) \quad (3.4)$$

$$\text{Solid: } 0 = k_{gj} a_p (1 - \varepsilon) (C_{gj} - C_{sj}) - r_j \quad \text{with } \dots r_j = \eta k_\infty \exp\left(-\frac{E_{act}}{RT_s}\right) RT_s C_{sj} \quad (3.5)$$

Boundary Conditions:

$$\begin{aligned} z = 0^+ \quad T_g - T_0 &= \frac{\varepsilon \lambda_{eff}^*}{(\rho C_p)_g u_g} \frac{\partial T_g}{\partial z} & C_{gj} - C_{gj0} &= \frac{\varepsilon D_{eff}^* C_l}{u_g} \frac{\partial y_{gj}}{\partial z} \\ z = L^+ \quad \frac{\partial T_g}{\partial z} &= 0 & \frac{\partial y_{gj}}{\partial z} &= 0 \end{aligned}$$

Dimension-less Model Equation

By introducing some dimension-less group we convert above the equations into dimensionless form as follows

Solid phase heat balance:

$$\frac{\partial \theta_s}{\partial \tau} = NTU_h (\theta_g - \theta_s) + Da \Delta \theta_{ad} \sum r_j^* H_j^* \quad (3.6)$$

Gas phase heat balance:

$$0 = -\frac{\partial \theta_g}{\partial \omega} - NTU_h (\theta_g - \theta_s) + \frac{1}{Pe_h^H} \frac{\partial^2 \theta_g}{\partial \omega^2} \quad (3.7)$$

Solid phase mass balance for component j:

$$0 = NTU_{mj} (y_{gj} - y_{sj}) - Dar_j^* \quad \text{Here } j=1 \quad (3.8)$$

Gas phase mass balance for component j:

$$0 = -\frac{\partial u_g y_{gj}}{\partial \omega} + \frac{1}{Pe_m} \frac{\partial^2 y_{gj}}{\partial \omega^2} - NTU_{mj} (y_{gj} - y_{sj}) \quad \text{Here } j=1 \quad (3.9)$$

Equation 3.6 is the solid phase heat balance. This heat balance will give variation of solid phase temperature with time which consists of two parts. The first part is concerned with the temperature increase by the difference in the temperature of solid and gas phase while part is related to the increase in temperature by reaction. It is to be noted that the second part takes place in catalytic monolith where reaction is taking place.

Likewise, Equation 3.7 is the gas phase heat balance which suggests the variation of temperature of gas with the height of reactor. Equation 3.8 is mass balance of solid phase whereby concentration difference and rate of reaction acts as the driving force. This equation gives the variation of the concentration with height of the reactor.

Boundary Conditions:

$$\omega = 0^- \quad \theta_g - \theta_0 = \frac{1}{Pe_h^H} \frac{\partial \theta_g}{\partial \omega} \quad y_{gj} - y_{gj}^0 = \frac{1}{Pe_m} \frac{\partial y_{gj}}{\partial \omega}$$

$$\omega = 1^+ \quad \frac{\partial \theta_g}{\partial \omega} = 0 \quad \frac{\partial y_{gj}}{\partial \omega} = 0$$

Dimensionless Groups

Dimensionless groups used in the above equations are as follows:

$$\theta_g = \frac{T_g}{T_0} \quad \omega = \frac{z}{L} \quad \tau = \frac{u_{g0} t}{\varepsilon L} \frac{1}{F}$$

$$H_j^* = \frac{H_j}{H_1} \quad y_{jg} = \frac{C_{jg}}{C_1^0} \quad y_{js} = \frac{C_{js}}{C_1^0}$$

$$\Delta \theta_{ad} = \frac{H_1 C_1^0}{(\rho C_p)_g T_0} \quad NTU_{mj} = \frac{k_{gj} a_p (1 - \varepsilon) L}{u_{g0}} \quad Pe_m = \frac{v_{g0} L}{D_{eff}}$$

$$NTU_h = \frac{\alpha a_p (1 - \varepsilon) L}{(\rho C_p)_g u_{g0}} \quad Da = \frac{r_1^0 L}{u_{g0} C_1^0} \quad \tau_c = \frac{u_{g0} t_c}{\varepsilon L} \frac{1}{F}$$

$$Pe_m = \frac{v_{g0} (\rho_0 C_p)_g L}{\lambda_{eff}} \quad F = \frac{(1 - \varepsilon) (\rho C_p)_s}{\varepsilon (\rho C_p)_g} \quad r_j^* = \frac{r_j}{r_1^0}$$

CHAPTER 4

SIMULATION OF THE MODEL

The heterogeneous model comprises a set of non-linear partial differential equations and non-linear algebraic equations which can only be solved numerically. In this part, a discussion of finite difference technique of numerical methods has been made which has been applied to solve these equations.

For the first derivative, a second order upwind scheme is used because it has better stability and is more accurate than a first order scheme and hence give more accurate results. The discretization at point m as given in Figure 4.1 can be written as,

$$\frac{dy}{dz} = \frac{y_{m-2} - h^2 y_{m-1} + (h^2 - 1)y_m}{h(h-1)\Delta z_m} \quad (4.1)$$

With $h = (z_m - z_{m-2}) / (z_m - z_{m-1})$ and $\Delta z_m = z_m - z_{m-1}$

For equally spaced grid

$$(z_m - z_{m-2}) = 2 * (z_m - z_{m-1})$$

Thus $h=2$, and hence,

$$\frac{dy}{dz} = \frac{y_{m-2} - 4y_{m-1} + 3y_m}{2\Delta z_m} \quad (4.2)$$

The second order derivative at point m is discretized as follows:

$$\frac{d^2 y}{dz^2} = 2 \frac{q y_{m-1} - (q+1)y_m + y_{m+1}}{q(q+1)\Delta z_m^2} \quad (4.3)$$

With $q = (z_{m+1} - z_m) / (z_m - z_{m-1})$

For an equidistance grid...

$$(z_{m+1} - z_m) = (z_m - z_{m-1})$$

Hence $q = 1$.

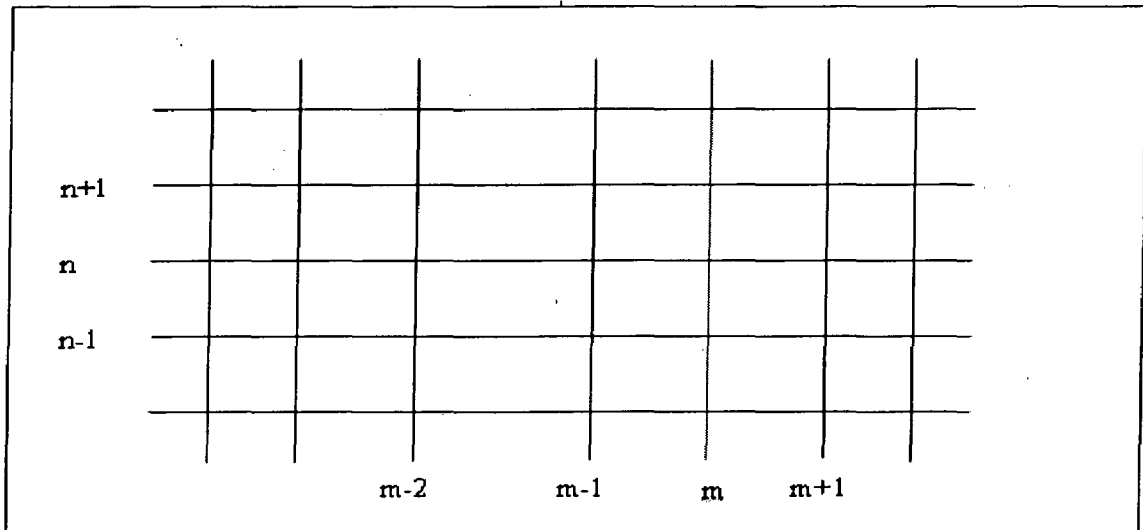
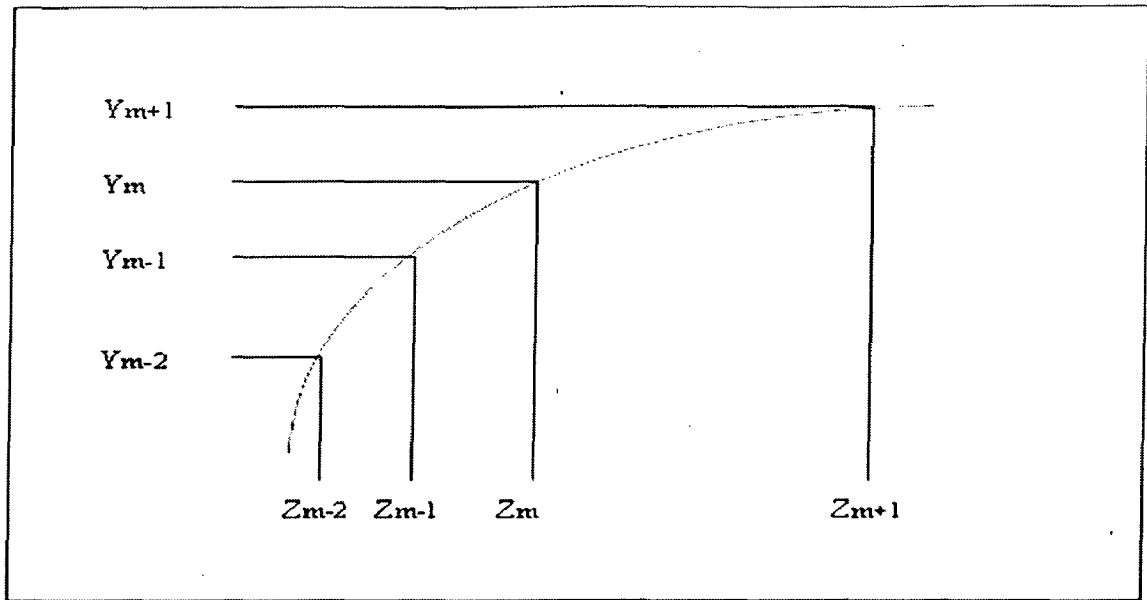
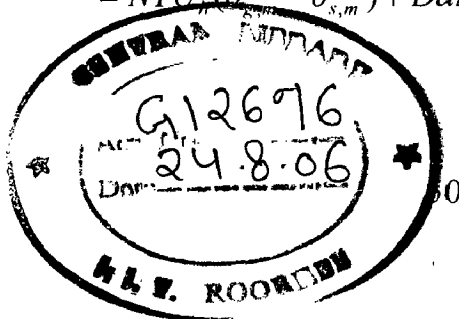


Figure 4.1: The finite difference method. A: Position of the grid points. B: The grid and the nomenclature.

It will be shown how the finite difference technique described above is applied to the dynamic heterogeneous model. Discretization of the solid phase heat balance with the aid of equation (4.2) gives

$$\frac{\theta_{s,m}^{n-1} - 4\theta_{s,m}^n + 3\theta_{s,m}^{n+1}}{2\Delta\tau} = NTU_n (\theta_{s,m}^{n+1} - \theta_{s,m}^n) + Da\Delta\theta_{ad} \sum r_{j,m}^{*,n+1} H_j^* \quad (4.4)$$



Which can be rewritten as,

$$\theta_{s,m}^{n+1} = \frac{\frac{4}{2\Delta\tau}\theta_{s,m}^{n-1} - \frac{1}{2\Delta\tau}\theta_{s,m}^{n-1} + NTU_h\theta_{g,m}^{n+1} + Da\Delta\theta_{ad}\sum r_{j,m}^{*,n+1}H_j^*}{\frac{3}{2\Delta\tau} + NTU_h} \quad (4.5)$$

With the aid of equation (4.1) and (4.3) the gas phase heat balance can be discretized as follows:

$$0 = -\frac{\theta_{g,m-2}^{n+1} - h^2\theta_{g,m-1}^{n+1} + (h^2 - 1)\theta_{g,m}^{n+1}}{h(h-1)\Delta\omega_m} - NTU_h(\theta_{g,m}^{n+1} - \theta_{s,m}^{n+1}) + \frac{2}{Pe} \frac{q\theta_{g,m-1}^{n+1} - (q+1)\theta_{g,m}^{n+1} + \theta_{g,m+1}^{n+1}}{q(q+1)\Delta\omega_m^2} \quad (4.6)$$

Rewriting the equation obtained on substituting equation (4.5) into equation (4.6) yields:

$$\begin{aligned} & \frac{1}{h(h-1)\Delta\omega_m} \theta_{g,m-2}^{n+1} - \left(\frac{h^2}{h(h-1)\Delta\omega_m} + \frac{2}{Pe} \frac{q}{q(1+q)\Delta\omega_m^2} \right) \theta_{g,m-1}^{n+1} \\ & \left(\frac{(h^2 - 1)}{h(h-1)\Delta\omega_m} + NTU_h \left[1 - \frac{NTU_h}{\frac{3}{2}\Delta\tau + NTU_h} \right] + \frac{2}{Pe} \frac{(q+1)}{q(1+q)\Delta\omega_m^2} \right) \theta_{g,m}^{n+1} \\ & - \frac{2}{Pe} \frac{1}{q(1+q)\Delta\omega_m^2} \theta_{g,m+1}^{n+1} = NTU_h \left(\frac{\frac{4}{2\Delta\tau}\theta_{s,m}^{n-1} - \frac{1}{2\Delta\tau}\theta_{s,m}^{n-1} + Da\Delta\theta_{ad}\sum r_{j,m}^{*,n+1}H_j^*}{\frac{3}{2\Delta\tau} + NTU_h} \right) \end{aligned} \quad (4.7)$$

Assuming first order reaction kinetics the mass balance for the solid phase and for each component can be written as follows

$$0 = NTU_{mj}(y_{jg,m}^{n+1} - y_{js,m}^{n+1}) - \frac{R_{j,m}^{n+1}}{r_1^0} y_{js,m}^{n+1} \quad (4.8)$$

$$\text{With } R_{j,m}^{n+1} = Dak_{\infty} e^{-\frac{E_{act}}{RT_{s,m}^{n+1}}} C_1^0$$

Rearranging the above equation gives

$$y_{j,s,m}^{n+1} = \frac{NTU_{mj} y_{jg,m}^{n+1} r_1^0}{NTU_{mj} r_1^0 + R_{j,m}^{n+1}} \quad (4.9)$$

Using Equations 4.1 and 4.3 the discretization of the gas phase mass balance for the component j can be obtained.

$$0 = u \frac{y_{g,m-2}^{n+1} - h^2 y_{g,m-1}^{n+1} + (h^2 - 1) y_{g,m}^{n+1}}{h(h-1)\Delta\omega_m} - NTU_{mj} (y_{jg,m}^{n+1} - y_{js,m}^{n+1}) + \frac{2}{Pe_m} \frac{q y_{g,m-1}^{n+1} - (q+1) y_{g,m}^{n+1} + y_{g,m+1}^{n+1}}{q(1+q)\Delta\omega_m^2} \quad (4.10)$$

Substitution of Equation 4.9 into Equation 4.10 and rearranging the expression obtained yields:

$$0 = \frac{u}{h(h-1)\Delta\omega_m} y_{jg,m-2}^{n+1} - \left(\frac{h^2 u}{h(h-1)\Delta\omega_m} + \frac{2}{Pe_m} \frac{q}{q(q+1)\Delta\omega_m^2} \right) y_{jg,m-1}^{n+1} + \left(\frac{(h^2 - 1)u}{h(h-1)\Delta\omega_m} - NTU_{mj} \left[1 - \frac{NTU_{mj}}{NTU_{mj} + \frac{R_{j,m}^{n+1}}{r_1^0}} \right] \right) y_{js,m}^{n+1} + \frac{2}{Pe_m q(1+q)\Delta\omega_m^2} y_{jg,m+1}^{n+1}$$

The model will now be used to study the changes in temperature and concentration in the reactor as a function of time and height. The results are discussed in the next chapter.

Chapter 5

RESULTS AND DISCUSSIONS

The behavior of an adiabatic packed bed reactor with periodic flow reversal has been studied by means of model calculations. The model was proposed by Boroskov *et al.* (1979) which had been further improved by van de Beld and Westerterp (1993). The packed bed acts as a regenerative heat exchanger due to high heat capacity of the solid phase and, thus an auto thermal process is possible even at very low contamination.

The model proposed by various authors is solved by different methods, e.g. van de Beld and Westerterp (1993) solution comprised of a set of partial differential equations transformed into non-linear ordinary differential equations and non-linear algebraic equation. Now these equations can be solved by initial guess in solid phase temperature profile in the equation and whole process is repeated until the difference between calculated and estimated value is smaller than a set value.

In this work, these equations are solved by using the programming features of MS EXCEL spread sheet. After solving the equations, different behavior of temperature in the solid bed and in gas phase are obtained. The behavior of the temperature obtained from the curves are investigated, such as, temperature of the gas rise in the first thermal monolith, then destruction of the volatile organic compounds takes place in catalytic monolith followed by decrease in temperature of the gas in second thermal monolith. On the other hand for the solid phase, temperature falls in first thermal monolith and rises in second thermal monolith due to heat exchange with gas phase.

Initially, the temperature of the gas was 300 K for which the dimensionless temperature was 1, which rose to 1.6 (Temperature = 480 K) before the entry of gas in the catalytic monolith. The dimensionless temperature of the gas declined to 1.2 at the exit of the thermal monolith which is equivalent to 360 K. The length of the first thermal monolith was 0.4 m while that of the second thermal monolith was also 0.4 m. On the other hand, the length of the catalytic monolith was 0.4 m. The catalytic monolith is further divided into two sections each of 0.2 m. The dimensionless concentration in the catalytic monolith reduced from 1.0 (2×10^{-3} mol/m³) to 0.25 (0.5×10^{-3} mol/m³) for the volatile organic compounds.

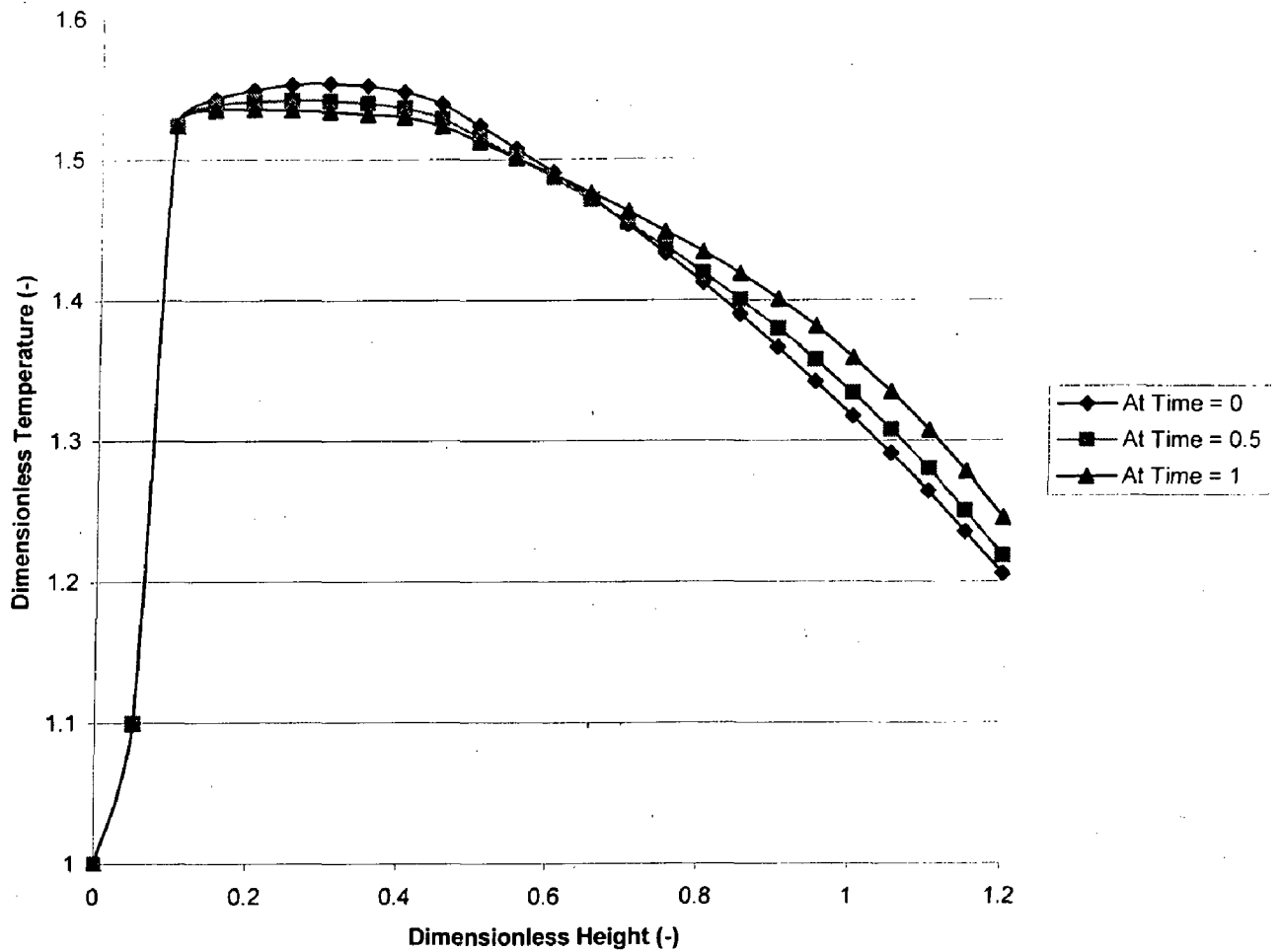


Figure 5.1: Graph between temperature of gas and height of the reactor (at Time = 0, 0.5, and 1) shows how temperature of gas increases and then decrease.

From Figure 5.1 it can be seen that temperature of the gas increases in first thermal monolith, no reaction take place in that part and temperature is increased only by the heat exchange between solid and gas phase. At the time of entry of gas, reactor temperature of the gas is low while temperature of the solid is fairly high which implies that heat exchange takes place from solid to gas phase. After attaining appreciable temperature, the gas enters the catalytic monolith where reaction takes place with the help of catalyst which reduces the amount of volatile organic compounds from the gas. The gas again enters the second catalytic monolith which results in further reduction in volatile organic compounds. On its entry into the second monolith, the temperature of the gas is more then temperature of solid which suggests that heat exchange takes place with the solid and, hence, reduction of the temperature of the gas. The gas coming out from the reactor is at 360 K.

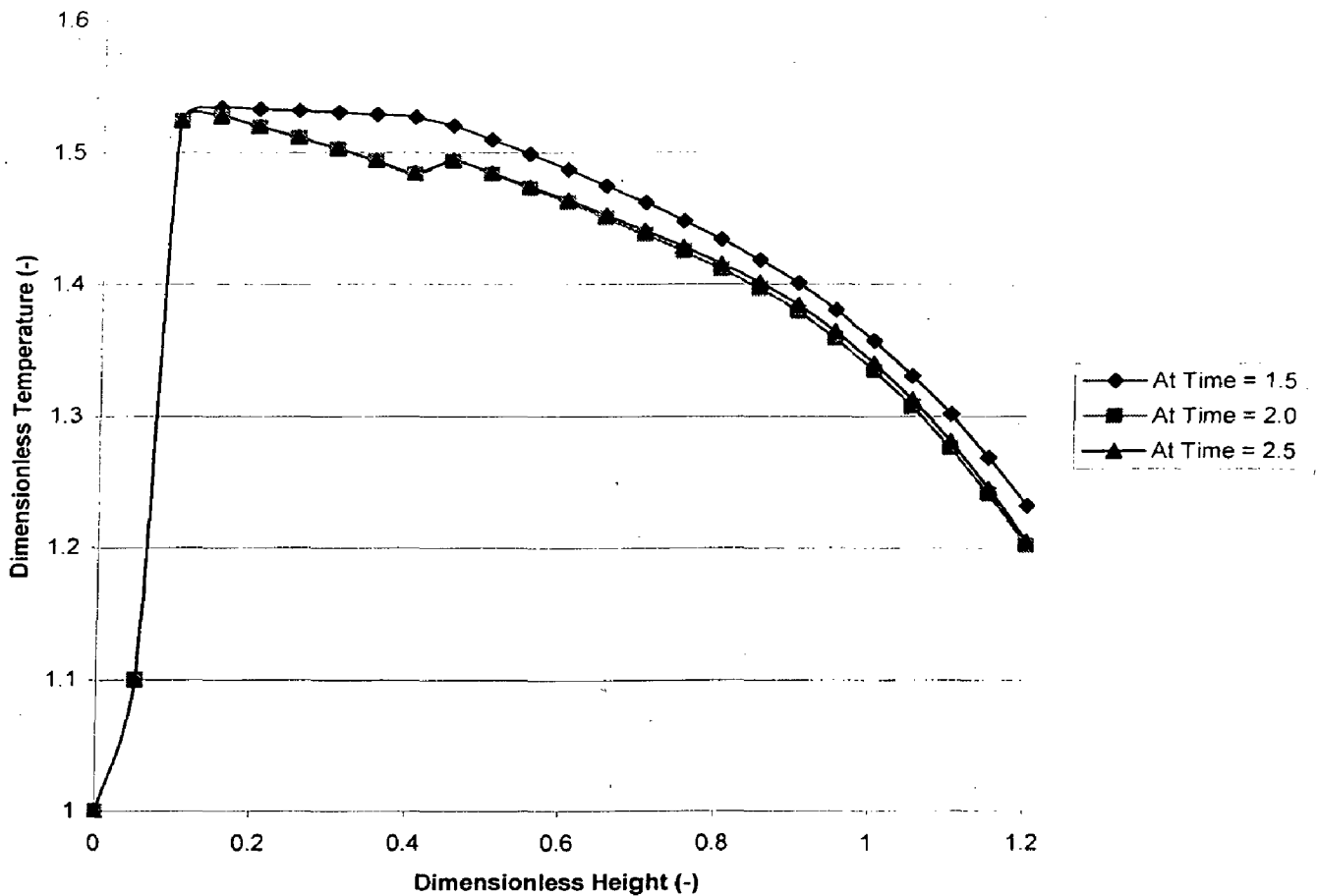


Figure 5.2: Graph between temperature of gas and height of the reactor (at Time = 1.5, 2.0, and 2.5) shows how temperature of gas increases and then decrease.

Figure 5.2 is almost same as Figure 5.1 with the only difference being the time. We can see a slight difference in the profile due to different time intervals. The temperature of gas decreases in second thermal monolith (0.8-1.2 m) because as gas enters this monolith its temperature is more then that of the solid phase, so heat transfer takes place from gas to the solid. The gas coming out from the reactor with low temperature and solid inside the reactor remains at high temperature. The heat exchange must be effective otherwise gas will come out from reactor at high temperature which will be against the public regulations. If economic consideration permits, additional coolers may be provided for cooling of gas emanating from the reactor. It is evident from the curves obtained that gas coming out from reactor is not at the room temperature which makes it mandatory to cool gas further by applying cooler or heat exchanger.

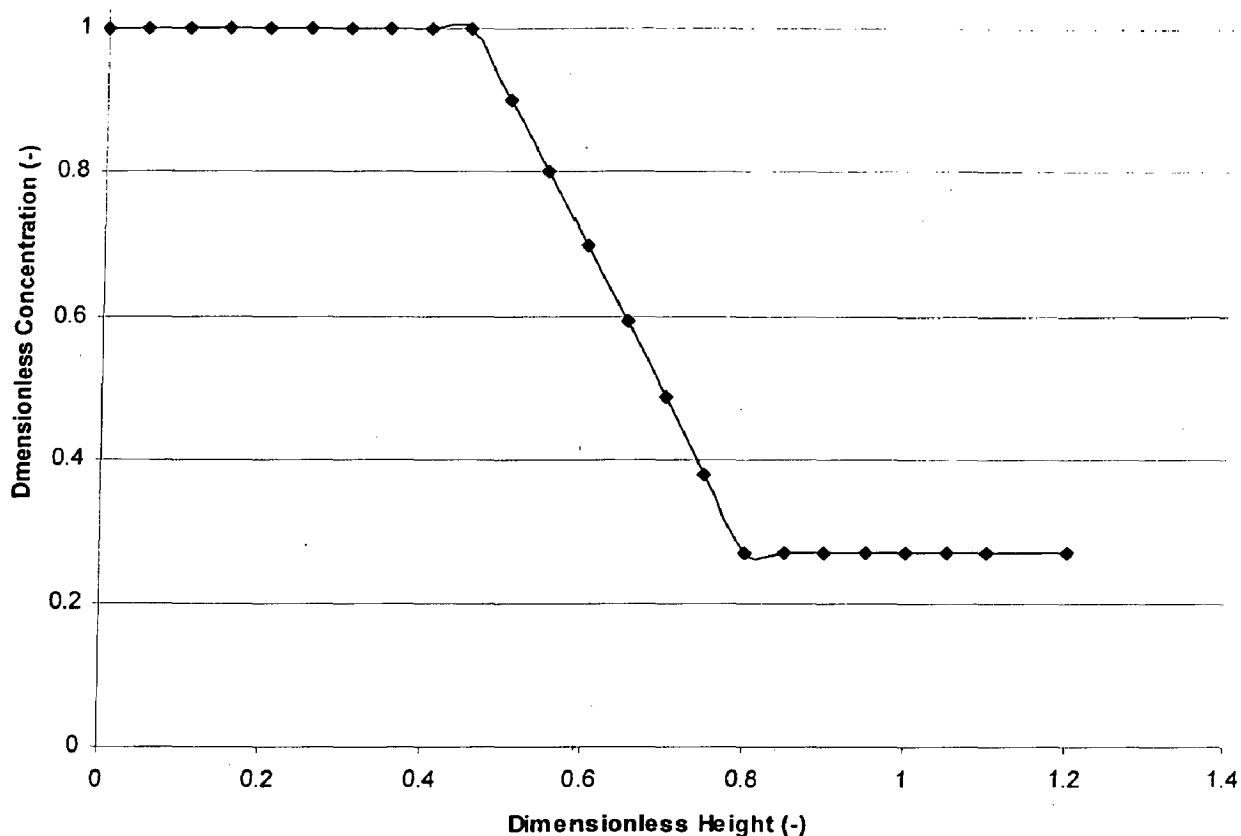


Figure 5.3: Graph between concentration of gas and Height of reactor, shows how concentrations of pollutant decrease.

From Figure 5.3 it can be seen that concentration of volatile organic compound have not changed in this monolith Since there is no catalyst in this part and hence no reaction takes place in this thermal monolith. When gas enters the catalytic monolith concentration of volatile organic compounds decreases rapidly because destruction of volatile organic compound takes place with the help of catalytic reaction and decrease as long as gas is in the catalytic part of the reactor. As it enters in the second thermal monolith, no further reaction take place and gas comes out at reduced concentration of volatile organic compounds. The dimensionless concentration in the catalytic monolith reduced from 1.0 ($2 \times 10^{-3} \text{ mol/m}^3$) to 0.25 ($0.5 \times 10^{-3} \text{ mol/m}^3$) for the volatile organic compounds.

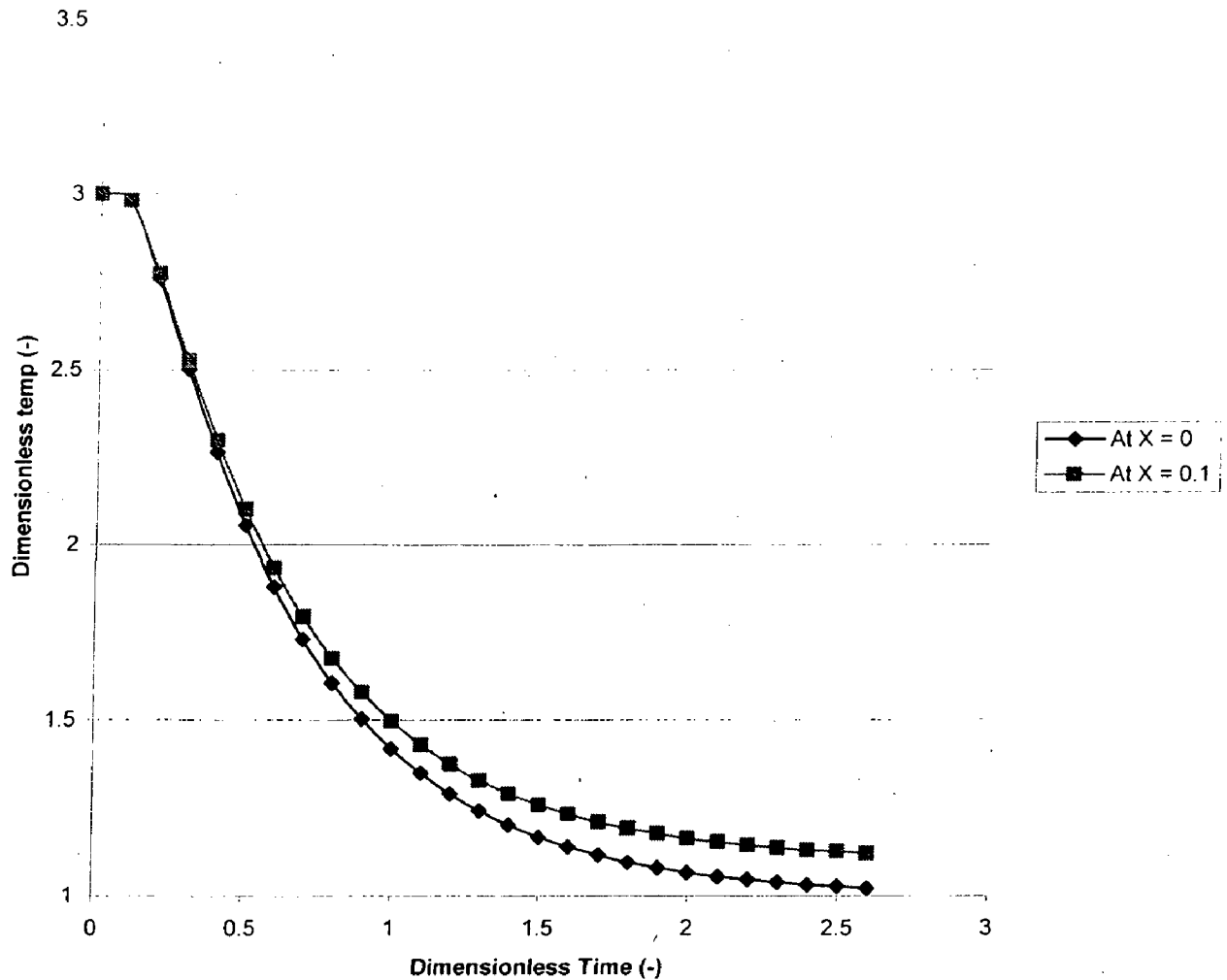


Figure 5.4: Graph between temperature of Wall (at $x=0$ and 0.1) and Time in first monolith in reactor, shows how temperature of wall decreases with time.

Figure 5.4 shows that the temperature of the solid in first thermal monolith decreases when heat exchange takes place with the gas in this part. The gas enters at room temperature and thermal monolith is at higher temperature which means that heat is transfer from solid to gas takes place. The temperature of gas is essentially increased but on the other hand temperature of the thermal monolith decreases with time. Since this graph is plotted between dimensionless time and dimensionless temperature, one can find out how much time is required to reduce the temperature up to the desired level.

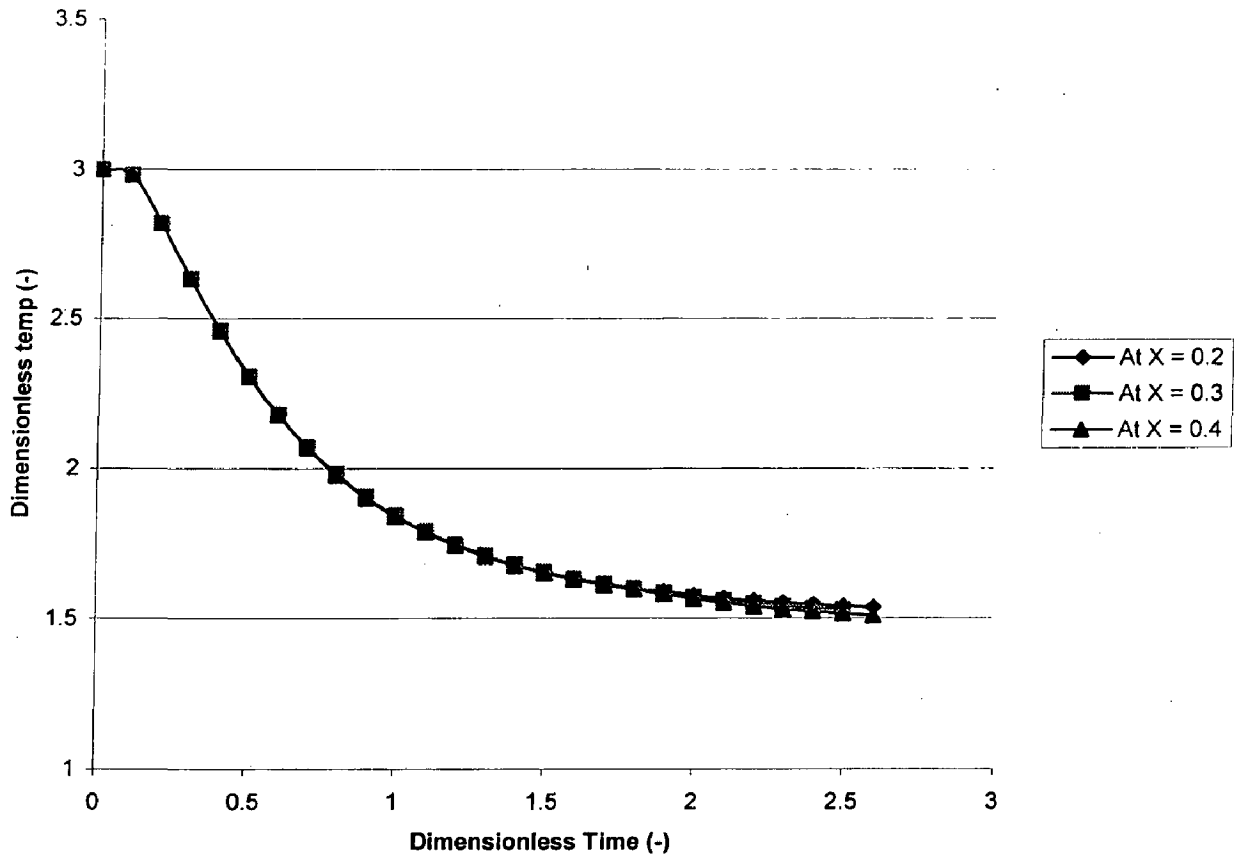


Figure 5.5: Graph between temperature of Wall (at $x=0.2, 0.3$ and 0.4) and Time in first monolith in reactor, shows how temperature of wall decreases with time.

Figure 5.5 is almost identical as Figure 5.4 the only difference being the different values of height of the reactor. There is little difference in the temperature profile at different height of reactor which may be attributed to low fluctuations in the feed condition and hence temperature profile varies accordingly.

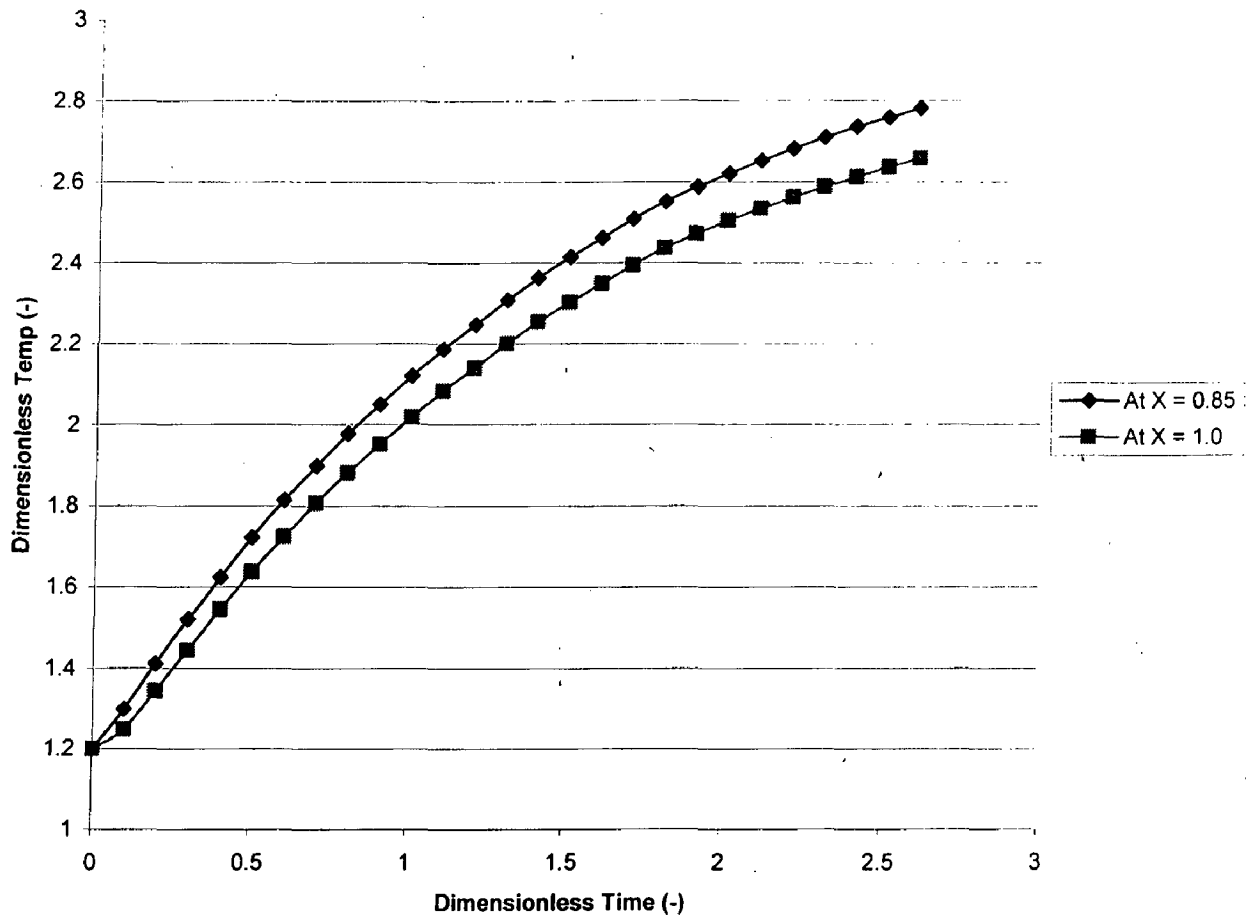


Figure 5.6: Graph between temperature of Wall (at $x=0.85$ and 1) and Time in second first monolith in reactor, shows how temperature of wall increase with time.

Figure 5.6 shows how temperature is increased in second thermal monolith. Since gas is at higher temperature when it enters in this region and thermal monolith is at low temperature, heat transfer takes place from gas to monolith. With this heat exchange gas comes out from the reactor at room temperature and thermal monolith remains at high temperature. This accommodated heat will be used in the next cycle when gas passes through this monolith and require heating.

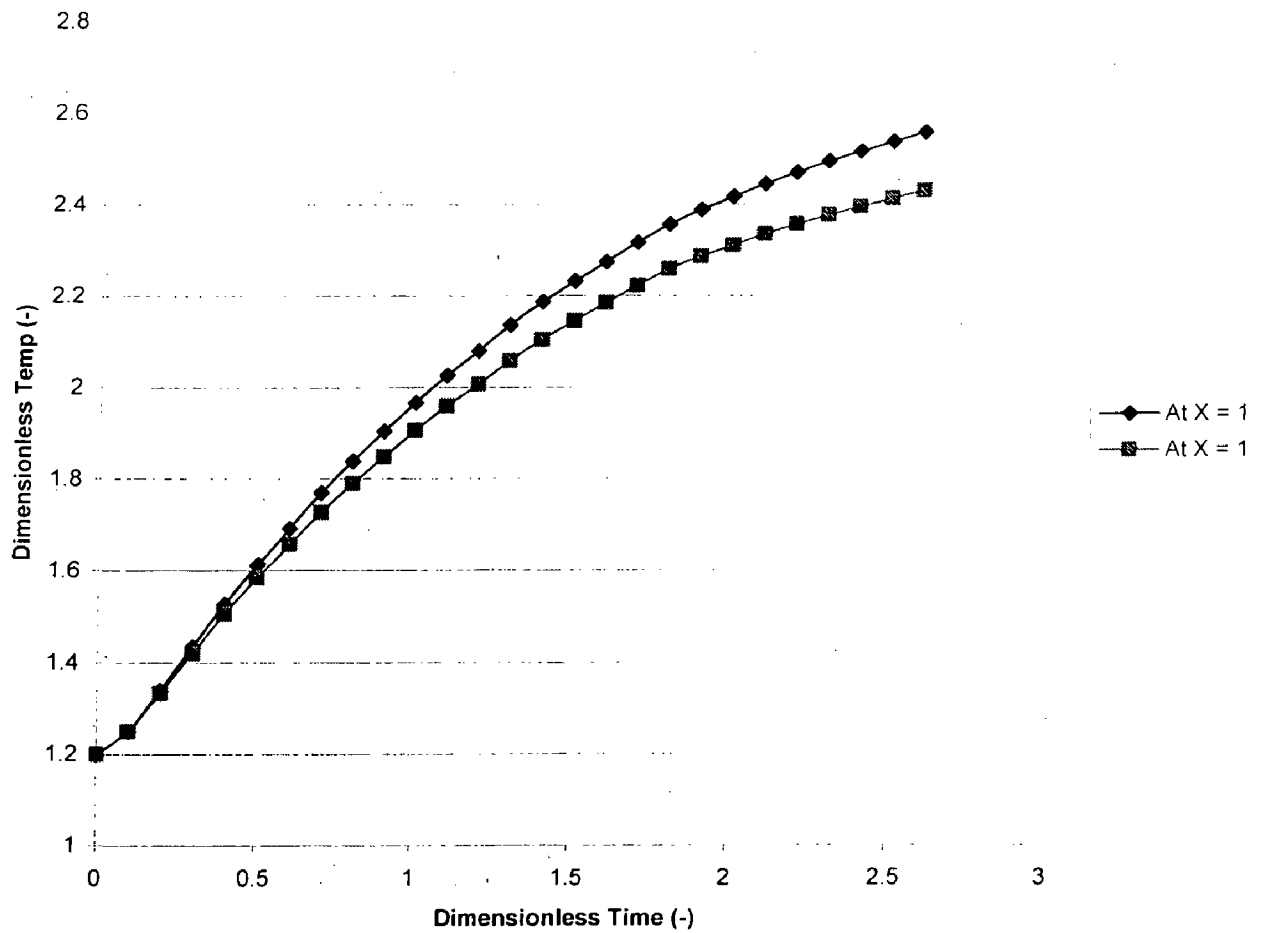


Figure 5.7: Graph between temperature of Wall (at $x=1.1$ and 1.2) and Time in second first monolith in reactor, shows how temperature of wall increase with time

Figure 5.7 is identical as Figure 5.6 with the only difference being the height of the reactor. It can be inferred that with slight change in the height of the reactor temperature profile also change slightly.

Chapter 6

CONCLUSIONS AND RECOMMENDATIONS

CONCLUSIONS

It is possible to purify waste air in a reverse flow reactor with auto thermal operation, in other words, without external supply of energy. To ensure auto thermal conditions, a minimum adiabatic temperature rise is essential which means that enough supply of feed or the components with high heat of combustion is required. A heterogeneous model has been derived to describe the behavior of the reactor. Although radial heat losses can not completely be excluded on small scale, by making use of evacuated jacket and several radiation shields the dynamics of the system are well defined and so heat loss are minimize. A reverse flow reactor can handle fluctuations in inlet condition well; complete conversion is still maintained for a long period of time after the feed concentration has dropped below the blow out value.

The reactor was operated successfully and high conversions of the contaminants were obtained without with out additional energy supply, provided that inlet concentrations are not too low.

RECOMMENDATIONS

In the proposed model, it is not possible to treat strongly polluted gas in this reactor. If we treat strongly polluted gas, there is always danger of the deterioration of precious catalyst. For the treatment of highly polluted gas, the inlet gas is diluted with the outlet gas (which is already treated) so that concentration of pollutant is decreased in the inlet gas volume, and the level of dilution i.e. recycle ratio is directly proportional to the level of pollution in the inlet gas. This will lead to reduction in temperature rise in catalytic monoliths and savings in the deterioration of precious catalyst. This strategy enables the treatment of very highly polluted gas whereas the proposed treatment strategy in the paper is beneficial up to a certain concentration of volatile organic compounds in the gas.

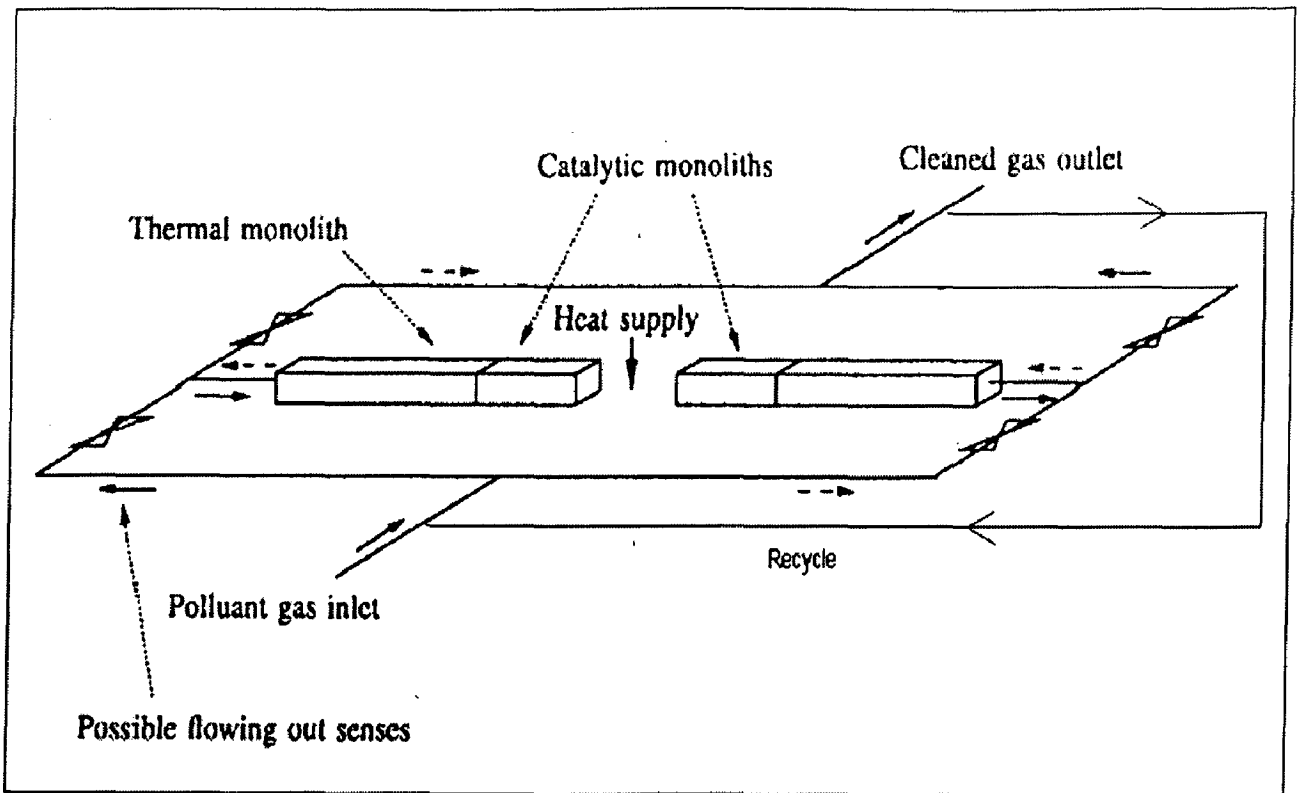


Figure 6.1: Improved principle scheme of catalytic reverse flow reactor

In Figure 6.1, a part of the outlet gas is recycled which results in the decrease in the inlet gas concentration of the pollutant. This recycle gas essentially increases the load on the reactor but dilutes the concentration of the pollutant in inlet gas and saves catalyst.

NOMENCLATURE

C	total molar concentration, mol m ⁻³
C _p	heat capacity, kJ kg ⁻¹ K ⁻¹
D _a	Damköhler number, dimensionless
D _{eff}	axial dispersion coefficient per unit void fraction, m ² s ⁻¹
a _v	particle external surface area, m ² m ⁻³
E _A	activation energy of reaction, kJ kmol ⁻¹
F	extraction factor, dimensionless.
h	dimensionless parameter for discretized equation.
H	heat of reaction kJmol ⁻¹
k _g	mass transfer coefficient m/sec
k _r	reaction rate constant, sec ⁻¹
NTU _h	number of heat transfer unit, dimensionless
NTU _m	number of mass transfer unit, dimensionless
Pe _h ^H	Peclet number heterogeneous
Pe _m	Peclet number axial mass transfer.
q	dimensionless parameter for discretized equations.
R	Gas constant, Kgmol ⁻¹ K ⁻¹
Re	Reynolds number, dimensionless
T	temperature, K
T _{max}	maximum temperature, K
T _{ad}	adiabatic temperature, K
t	time, sec
t _c	cycle Time, sec
u	superficial gas velocity, ms ⁻¹
x	conversion, dimensionless
y	dimensionless concentration
z	axial coordinate, m

GREEK SYMBOLS

α	Heat transfer coefficient for particle, kW/m ² K
ε	Bed porosity, dimensionless
ρ	density, kg/m ³
θ	dimensionless temperature
$\theta_{plateau}$	dimensionless plateau temperature
$\Delta\theta_{ad}$	dimensionless adiabatic temperature
ω	dimensionless axial coordinate
τ	dimensionless time
τ_c	dimensionless cycle time

SUBSCRIPT

g	gas
j	component j
m	spatial index for discretized equation
M	number of grid point
s	solid
0	initial condition

SUPERSCRIPT

H	heterogeneous model
PH	pseudo-homogeneous model
m	spatial index for discretized equation
M	number of grid point
N	time index for discretized equation
0	initial condition
•	dimensionless

REFERENCES

1. Agarwal, S.K., Spievy, J.J. (1993), Economic effects of catalytic deactivation during VOC oxidation, *Env. Provr.*, **12**, 182-185.
2. Aubé, F, and H. Sapoundjiev (2000), Mathematical model and numerical simulations of catalytic flow reversal reactors for industrial applications, *Computers and Chemical Engineering*, **24**, 2623-2632.
3. Boroskov, G.K., Matros, Yu.Sh., Ivanov, A.G., (1986), Utilization of the heat of catalytic combustion of low calorie gaseous mixtures by reversing the direction of their input, *Dokaly Chem.Tech.*, **288**, 55-59.
4. Chumachenko, V. A.; Matros, Yu. Sh. (1990) Catalytic purification of gases from organic substances under unsteady-state conditions; result and predictions. *Proceedings of International Conference*, Novosibirsk, U.S.S.R., June 5-8, 1990; VSP BV: Utrecht, The Netherlands, 605-612.
5. Cittadini, M., Vanni, M., Barresi, A.A., Baldi, G., (2001), Reverse-flow catalytic burners: response to periodical variations in the feed, *Chemical Engineering Science*, 2001, **56**, 1443-1449.
6. Cunill, F., van de Beld, L., Westerterp, K.R. (1997), Catalytic combustion of very lean mixtures in a reverse flow reactor using an internal electrical heater, *Ind. Eng. Chem. Res.*, **36**, 4198-4206.
7. Dufour, P., and Touré, Y, (2004), Multivariable model predictive control of a catalytic reverse flow reactor, *Chemical Engineering Science*, **28**, 2259-2270.
8. Eingenberger, G., & Nieken, U. (1988). Catalytic combustion with periodic flow reversal. *Chemical Engineering Science*, **43**, 3023-3030.
9. Gawdzik, A., Rakowski, L., (1988), dynamic properties of the adiabatic tubular reactor with switch flow, *Chemical Engineering Science*, **43**, 3023-3030.
10. Gosiewski, K., & Sztaba, R. (1990). In Yu. Sh. Matros, Unsteady State Processes in Catalysis, VPS BV, Utrecht, 629-635

11. Haynes, T. N., Georgakis, C. G., & Caram, H. S, (1995), The design of reverse flow reactors for catalytic combustion systems. *Chemical Engineering Science*, **50**, 401–416.
12. Hydrocarbon Processing's Environmental processes, (1993), *Hydrocarbon Processing*, 67-105.
13. Jeong, Y. O., Luss, D., (2003), Pollutant destruction in a reverse flow chromatographic reactor *Chemical Engineering Science*, **58**, 1095-1102.
14. Matros, Yu. Su., (1990), Mathematical modeling of chemical reactors-Development and implementation of novel technologies, *Angew. Chem. Int. Ed. Engl.*, **29**, 1235-1245.
15. Matros, Yu. Sh., 1990, Performance of catalytic processes under steady state conditions, Unsteady state processes in catalysis: proc. Of international conference, 5-8 June 1990, Novosibirsk, U.S.S.R., V.S.P. B.V, Utrecht, The Netherlands, 131-164.
16. Matros, Yu. Sh.; Noskov, A.S.; Chumachenko, V. A.; Goldman, O. V. (1988), Theory and application of unsteady-state catalytic detoxication of effluent gases from dioxide, nitrogen oxides and organic compounds. *Chemical Engineering Science*, **43**, 2061-2066.
17. Matros, Yu. Sh., Bonimovich, G.A., (1996) Reverse-flow operation in fixed bed catalytic reactors, *Catalysis reviews*, **38**, 1-68.
18. Mitri, A., Neumann, D., Liu, T., Vesper, G, (2004), Reverse flow reactor operation and catalyst deactivation during high temperature catalytic partial oxidation, *Chemical Engineering Science*, **59**, 5527-5534.
19. Neumann, D., and Vesper, G. (2004), Catalytic partial oxidation of methane in a high temperature reverse flow reactor, *The American Institute of Chemical Engineers Journal*, **51**, 210-223.
20. Nieken, U., Kolios, G., & Eigenberger, G. (1995). Limiting cases and approximate solutions for fixed-bed reactors with periodic flow reversal. *The American Institute of Chemical Engineers Journal*, **41**, 1915-1925.
21. Riel, P.H. van, (1991) Concentratie koolwaterstoffen in afgassen opvoeren met actief koolvezel, *Energie and milieutechnologie*, No. **11-12**, 6-20.

22. Sapundzhiev, C.; Groves, G.; Elenkov, D. (1991) non steady-state catalytic decontamination of waste gases. *Chemical Engineering Technology*, **14**, 209-212.
23. Tullilah, M.B., Alajem, E., Gal, R., Sheintuch, M, (2003), Flow-rate effects in flow-reversal reactors: experiments, simulations and approximations. *Chemical Engineering Science*, **58**, 1135-1146.
24. van de Beld, L., Bijl, M.P.G., Reinders, A., Werf, B.V., Westerterp, K.R. (1994), The catalytic oxidation of organic contaminants in packed bed reactor, *Chemical Engineering Science*, **49**, 4361-4373.
25. van de Beld, L., Borman, R.A., Derkx, O.R., van Woezik, B. A. A., Westerterp, K.R. (1994), Removal of volatile organic compounds from polluted air in a reverse flow reactor: An experimental study, *Ind. Eng. Chem. Res.*, **33**, 2946-2956.
26. van Sint Annaland, M., Kuipers, J.A.M., van Swaaij, W.M.P, (2001), Safety analysis of switching between reductive and oxidative conditions in a reaction coupling reverse flow reactor, *Chemical Engineering Science*, **56**, 1517-1524.
27. van Sint, and Nijssen, R.C, (2002), A novel reverse flow reactor coupling endothermic and exothermic reactions: An experimental study, *Chemical Engineering Science*, **57**, 4967-4985.
28. Viecco, G.A., Caram, H.S. (2002), The spherical reverse flow reactor, *Chemical Engineering Science*, **57**, 4005-4025.
29. Westerterp, K.R., (1992) Multifunctional reactors, *Chemical Engineering Science*, **47**, 2195-2206.